Draft

Date: **Apr. 2, 2009**
Not approved for public release

Proceedings of PVP2009
2009 ASME Pressure Vessels and Piping Division Conference
July 26-30, 2009, Prague, Czech Republic

PVP2009-77974

DESIGN OF A PYTHON-BASED PLUG-IN FOR BENCHMARKING PROBABILISTIC FRACTURE MECHANICS COMPUTER CODES WITH FAILURE EVENT DATA (*)

Jeffrey T. Fong
Mathematical & Computational Sciences Division
National Institute of Standards & Technology (**NIST**)
Gaithersburg, MD 20899-8910 USA
fong@nist.gov

Roland deWit
Metallurgy Division
National Institute of Standards & Tech. (**NIST**)
Gaithersburg, MD 20899 USA
deWit@nist.gov

Pedro V. Marcal
MPave Corp.
3606 Calico Ranch Gate
Julian, CA 92036 USA
marcalpv@cox.net

James J. Filliben
Statistical Engineering Division
National Institute of Standards & Tech. (**NIST**)
Gaithersburg, MD 20899-8980 USA
filliben@nist.gov

N. Alan Heckert
Statistical Engineering Division
National Institute of Standards & Technology (**NIST**)
Gaithersburg, MD 20899-8980 USA
alan.heckert@nist.gov

Stephen R. Gosselin
Scandpower Risk Management, Inc.
1331 Lamar St., Suite 1270
Houston, TX 77010 USA
srg@scandpower.com

ABSTRACT

In a 2007 paper entitled "Application of Failure Event Data to Benchmark Probabilistic Fracture Mechanics (PFM) Computer Codes" (Simonen, F. A., Gosselin, S. R., Lydell, B. O. Y., Rudland, D. L., & Wikowski, G. M. *Proc. ASME PVP Conf., San Antonio, TX,* Paper PVP2007-26373), it was reported that the two benchmarked PFM models, PRO-LOCA and PRAISE, predicted significantly higher failure probabilities of cracking than those derived from field data in three PWR and one BWR cases by a factor ranging from 30 to 10,000. To explain the reasons for having such a large discrepancy, the authors listed ten sources of uncertainties: (1) Welding Residual Stresses. (2) Crack Initiation Predictions. (3) Crack Growth Rates. (4) Circumferential Stress Variation. (5) Operating temperatures different from design temperatures. (6) Temperature factor in actual activation energy vs. assumed. (7) Under reporting of field data due to NDE limitations. (8) Uncertainty in modeling initiation, growth, and linking of multiple cracks around the circumference of a weld. (9) Correlation of crack initiation times and growth rates. (10) Insights from NUREG/CR-6674 (2000) fatigue crack growth models using conservative inputs for cyclic strain rates and environmental parameters such as oxygen content. In this paper we design a Python-based plug-in that allows a user to address those ten sources of uncertainties. This approach is based on the statistical theory of design of experiments with a 2-level factorial design, where a small number of runs is enough to estimate the uncertainties in the predictions of PFM models due to some combination of the source uncertainties listed by Simonen et al (PVP2007-26373).

Keywords: Aging structures; ANLAP; artificial intelligence; crack initiation; crack propagation; DATAPLOT; design of experiments; failure event database; fatigue; flaw detection; fracture mechanics; information extraction; inservice inspection; life extension; material property database; mathematical modeling; NDE database; nuclear power plants; nuclear safety; petro-chemical plants; PRAISE; probabilistic fracture mechanics; PD-UP, PYTHON; residual stresses; risk-informed analysis; statistical analysis; uncertainty analysis.

(*) Contribution of the U.S. National Institute of Standards and Technology (NIST). Not subject to copyright.

Disclaimer: The views expressed in this paper are strictly those of the authors and do not necessarily reflect those of their affiliated institutions. The mention of names of all commercial vendors and their products is intended to illustrate the capabilities of existing products, and should not be construed as endorsement by the authors or their affiliated institutions.

I. INTRODUCTION

Over the last thirty years following the 1979 nuclear accident at Three Mile Island [1][1], much research has been done on the development and application of inservice inspection (ISI), failure event databases, and risk-informed fatigue modeling of defect management for pressure vessels and piping [2-37]. The good news is reflected in Figure 1, where Pietrangelo [38, 39] showed in 2008 that the U.S. nuclear powerplant average capacity factor increased from 66 % in 1990 to an astonishingly high 91.8 % in 2007, resulting in a huge 39% increase in the annual energy production of 104 power reactors over a span of 17 years -- from 580 to 807 billion kilowatt-hours per year -- without building since 1979 a single new commercial reactor. On the other hand, some not-so-good news was hinted in 2004 by Teather [40], who reported that

> " . . . The fleet of reactors in the U.S. is aging, however, and many are now applying for licences to extend their lives.
> "By the end of this year (2004), a third of the existing plants, built to last for 40 years, will have applied for licences to continue operating for another 20."

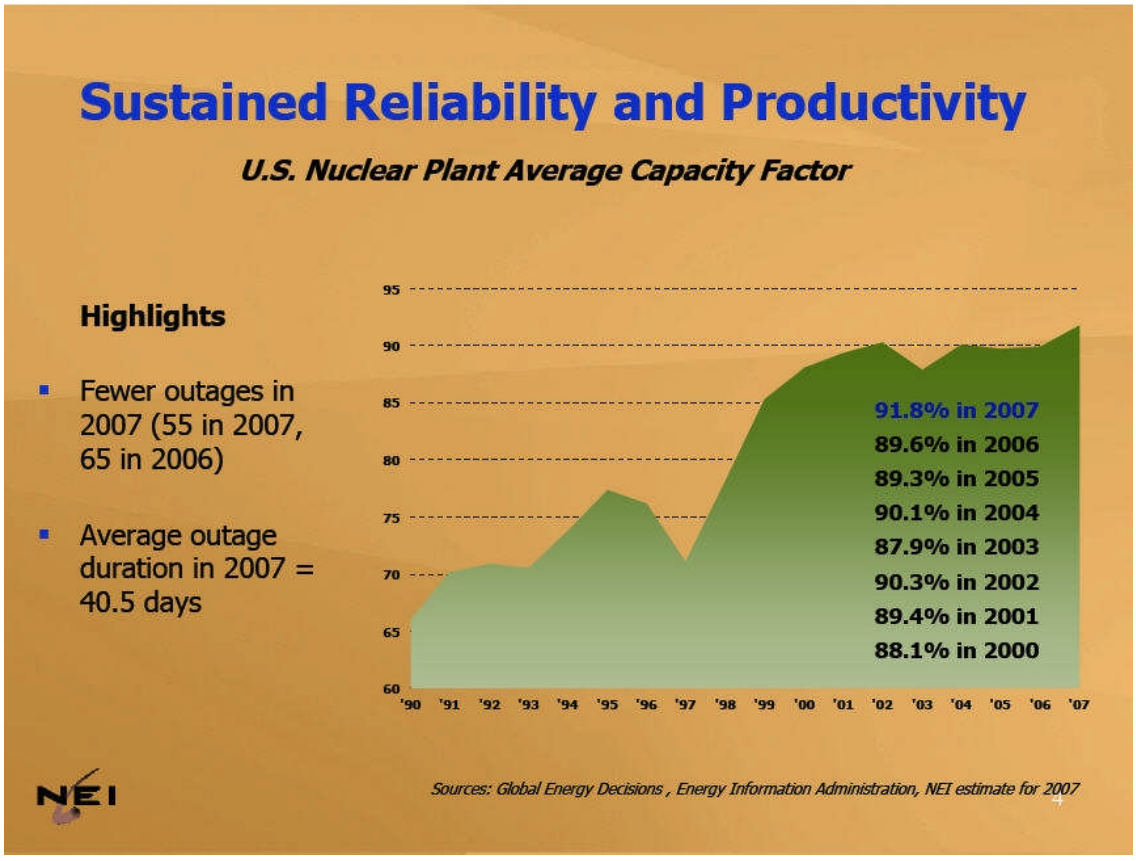

Figure 1. U.S. Nuclear Plant Average Capacity Factor (1990 - 2007), after Pietrangelo [39].

[1]Figures in square brackets denote references listed at the end of this paper.

I. INTRODUCTION (CONT'D)

The problem of maintaining and safely operating an aging equipment or structure is not unique to a nuclear powerplant, as reported recently in a New York Times article by Cooper [41]:

> " . . . More than a quarter of the nation's bridges are structurally deficient or functionally obsolete. Leaky pipes lose an estimated seven billion gallons of clean drinking water every day. And aging sewage systems send billions of gallons of untreated wastewater cascading into the nation's waterways each year."

Getting back to the highly-researched and heavily-regulated problem of permitting a 40-year-old nuclear power plant to operate for another 20 years, we show in Fig. 2 a specific result of a Probabilistic Fracture Mechanics (PFM) simulation using a computer code named "PC-PRAISE" for the surge-line elbow of a Combustion Engineering plant in terms of probabilities of crack initiation and through-wall cracks as a function of time (after a 2000 NUREG/CR6674 report by Khaleel, Simonen, Phan, Harris, and Dedhia [17]). In that report, the authors [17, p. 9.7] stated:

> " . . . It is seen that cracks initiate rather early in the plant life. There is about a 50-percent probability of initiating a fatigue crack after only 10 years of operation.
> " . . . Over this 10 years, about 50 percent of these initiated cracks are predicted to grow to become leaking cracks.
> " . . . The frequency of through-wall cracks (lower curve) increases significantly over this 10 years and then remains relatively constant over the remainder of the 60-year plant life."

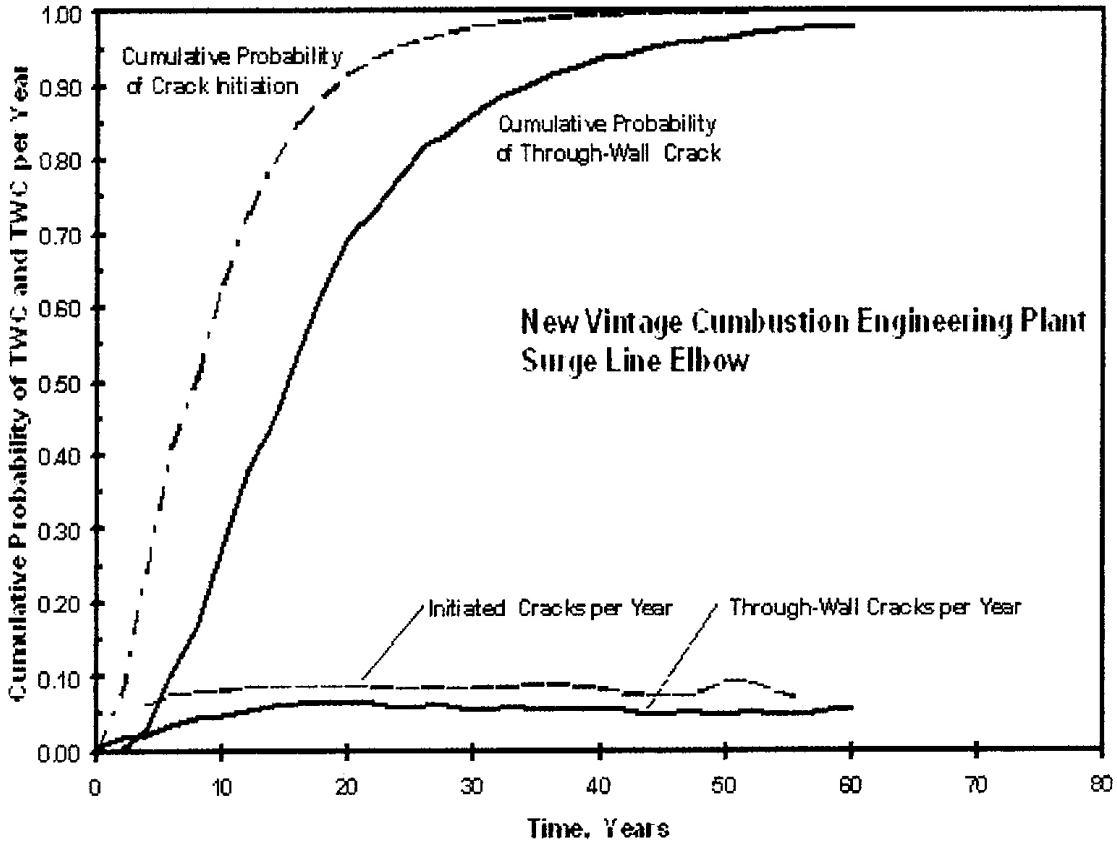

Figure 2. Calculated Probabilities of Crack Initiation and Through-Wall Crack for the Surge-Line Elbow of the Newer Vintage Combustion Engineering Plant (after Khaleel, Simonen, Phan, Harris, and Dedhia [17]).

I. INTRODUCTION (CONT'D)

In that same report [17, p. 10.1], the authors concluded that,

" . . . The calculations gave a wide range of failure probabilities for the selected components, with some components having end-of-life probabilities of through-wall cracks of nearly 100 percent and others with probabilities of less than 10^{-6}.

" . . . It is recognized that there are uncertainties in these calculated failure probabilities and core damage frequencies. Sources of the uncertainties come from assumptions made in the fracture mechanics and probabilistic risk analysis models themselves and from the inputs to the models.

" . . . In particular, the inputs for cyclic stresses were based on design-basis data, which could differ from the stresses occurring during the actual plant operation."

On the role of failure data in plant aging management, Chockie and Gregor [29] presented in 2008 an assessment and a more rational approach to the complex problem of failure event and inservice inspection data collection, analysis, interpretation and life extension decision making:

" . . . After almost forty years there is a vast amount of data on operational performance of nuclear plants and their systems, structures, and components (SSCs).

" . . . By understanding some of the key **limitations of the data sources**, more effective use can be made of the information gained from the analysis of the data.

" . . .This operational performance data and the resulting information, in combination with an **economic assessment of the benefits and costs** of various options, is essential for effective aging management and life extension decisions of the nuclear power plants."

*(**boldface** furnished by authors of this paper.)*

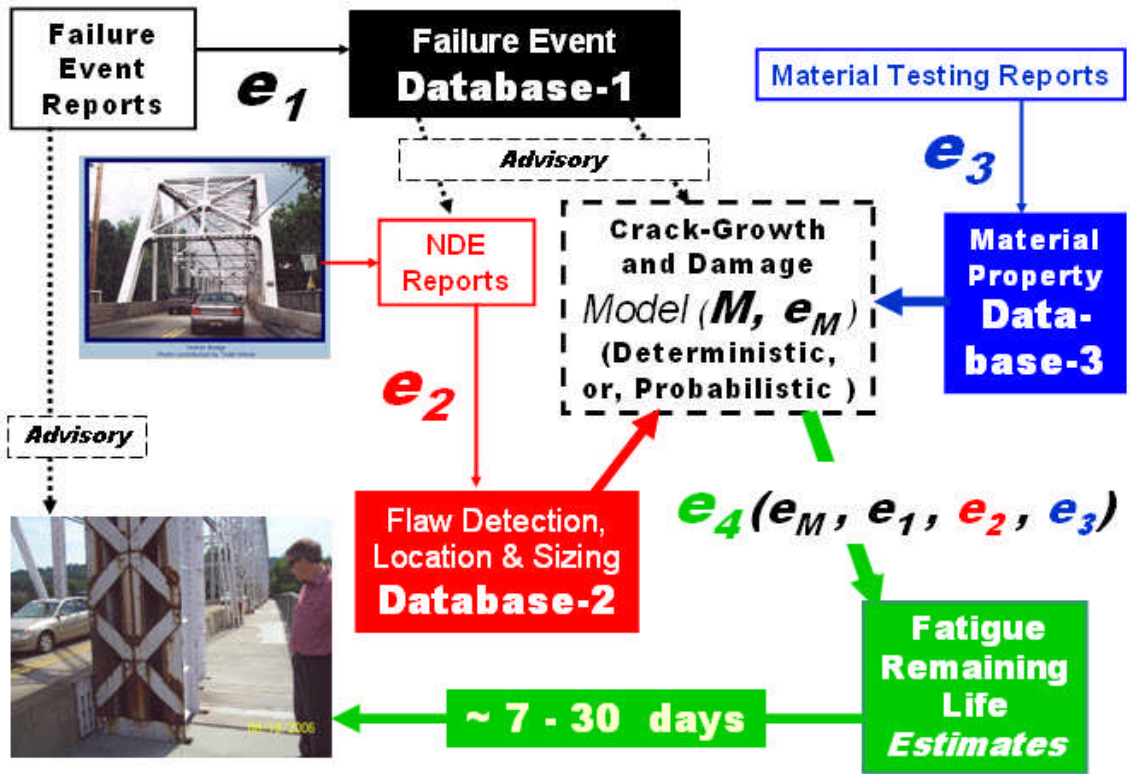

Figure 3. A conceptual representation (after Fong and Marcal [30] and Fong, Ranson, Vachon, and Marcal [33]) of the information flow plus the uncertainties and potential errors associated with and inherent in Failure Event Database-1 (*Uncertainty-1, or, e_1*), Flaw Detection, Location & Sizing Database-2 (*Uncertainty-2, or, e_2*), Material Property Database-3 (*Uncertainty-3, or, e_3*), Deterministic or Probabilistic Damage Models (*Uncertainty-M, or, e_M*) and Remaining Life Estimates (*Uncertainty-4, e_4*). Photo at the upper left corner is from the 70-year-old Jonathan Hulton Bridge, built in 1909, of Pittsburgh, PA, courtesy of reference [42]. Photo at the lower left corner was taken by the first author (Fong) during a site visit to the bridge in 2006.

I. INTRODUCTION (CONT'D)

As shown in Figure 3 (after Fong and Marcal [30] and Fong, Ranson, Vachon, and Marcal [33]), the complex flow of information, both qualitative and quantitative, from (1) failure event reports, (2) ISI and NDE reports, (3) material testing reports, (4) computer modeling simulations, and (5) remaining life estimates for decision making, is associated with all sorts of uncertainties and potential errors due to data collection, interpretation, analysis, and modeling. For our purposes here, let us associate each of the first three information categories with the notion of a database plus a generic term of uncertainty as follows:

DB-1: Failure Event Database with uncertainty e_1 (global and local).

DB-2: Inservice Inspection (ISI) and NDE Database with uncertainty e_2 (local).

DB-3: Material Property Database with uncertainty e_3 (both global and local).

Two more sources of uncertainty, which should be but had not been included yet in our representation map of Figure 3, need to be identified and discussed. In Table 1, we introduce a notation for all factors suspected of contributing uncertainties to a class of fatigue life prediction models of an aging structure:

Table 1. A List of Uncertainty-Contributing Factors in 5 Categories of Databases

Nature of Factors	*Symbol of Factors*	*Database (Uncertainty)*
Failure mechanisms	F_i , $i = 1, 2, \ldots n_F$	**DB-1** (e_1)
NDE flaw geometry	N_j , $j = 1, 2, \ldots n_N$	**DB-2** (e_2)
Material property	M_k , $k = 1, 2, \ldots n_M$	**DB-3** (e_3)
Loadings and constraints	L_u , $u = 1, 2, \ldots n_L$	*Important, but not treated here.*
Physical-chemical composition (incl. dimensions) *treated here.*	P_v , $v = 1, 2, \ldots n_P$	*Important but not*

It is worth noting that engineers who manage the integrity of an aging structure need to learn how to collect, analyze, and interpret both the "global" and the "local" types of information about the "health" of that structure, much as the way a medical doctor has been doing for years in treating an elderly patient using published health statistics (global) from a well-defined population, and the hematology, blood chemistry, bone density, and urinalysis data (local) of a patient over a period of time.

In Figure 3, we have also introduced a notation for a mathematical model, M. In general, M is made up of (1) governing equations based on known or plausible physical, chemical, and biological laws, (2) geometric parameters, material property coefficients and physical constants (also known as factors), (3) loadings and constraints in the form of initial and boundary conditions, and (4) discretization and computational algorithm parameters including software and hardware specifics if the model is solved numerically on a computer.

If we consider M as a black box, and if we know that the governing equations are not fully understood and the list of parameters that define M contains some not yet identified in Table 1, it is incumbent upon us to introduce another uncertainty source, e_M, that is intrinsic to M and collectively represents all additional uncertainties inside the black box.

In Figure 3, we have also introduced a result uncertainty, e_4, that should depend on the four source uncertainties identified so far, i.e.,

e_1 - associated with ***failure event database-1 ,***

e_2 - associated with ***flaw detection/location/sizing-2 ,***

e_3 - associated with ***material property database-3 ,***

e_M - associated with ***crack-growth/damage modeling ,***

such that the fatigue remaining life estimates of an aging structure will have a result uncertainty denoted by

e_4 - associated with ***remaining life estimates .***

In other words, we assume the existence of an explicit (or implicit as the case may be) functional representation of e_4 as follows:

$$e_4 = f(e_M, e_1, e_2, e_3, \ldots), \qquad (1)$$

where the three dots represent uncertainties due to those factors listed in Table 1 but not treated in this paper.

I. INTRODUCTION (CONT'D)

To address and estimate the five types of uncertainties identified above, we have developed an approach based on the statistical theory of design of experiments (see, e.g., Box, Hunter, and Hunter [43], Croarkin, et al. [44]) and implemented with a public-domain software package named DATAPLOT (see Filliben and Heckert [45], Fong, et al. [46-49]). To report our findings, we have prepared a series of four papers for presentation at the July 27-30, 2009 ASME PVP Conference in Prague. Those four papers are:

- e_1 - Fong-Marcal-Yamagata [50].
- e_2 - Fong-Marcal-Hedden-Chao-Lam [51].
- e_3 - Fong-Marcal [52].
- e_M and e_4 - Fong-deWit-Marcal-Filliben-Heckert-Gosselin [*This paper*].

The goals of this paper are two-fold:

(a) To present a summary of the findings of the first three papers [50, 51, 52] as an introduction to this paper.

(b) To present an uncertainty estimation plug-in tool named PD-UP [49, 53] with four examples of learning something about the function f in Eq. (1) such that one may rank the relative importance of all possible factors and their interactions as contributors to the result uncertainty, e_4, and, if two or three factors were found "dominant," one might use a simple linear least square fit algorithm to estimate e_4.

In **Sect. II**, we address the problem of better managing a failure event database, ***DB-1*** , and estimating its e_1 by briefly describing a new artificial intelligence (AI) tool named ANLAP (abbrev. for automatic natural language abstracting and processing). As described more fully in [50] by Marcal, Fong, and Yamagata, this information extracting tool and its computer linkage with statistical and finite element analysis packages may minimize chances of human errors when a time-critical operating decision had to be made involving the mining of a massive amount of technical reports and a probabilistic modeling of the aging behavior of a complex system such as a nuclear power plant.

In **Sect. III**, we address the problem of better managing an ISI and NDE database, ***DB-2*** , and estimating its e_2 by briefly describing the use of a DEX-based and DATAPLOT-implemented 10-step analysis tool due to Filliben and Heckert [45]. Again, as described more fully in [51] by Fong, Marcal, Hedden, Chao, and Lam, this analysis tool allows a user to rank the relative importance of field-based NDE processing factors and obtain a quantitative estimate of the uncertainty of ISI-generated information such as crack detection, location, and sizing.

In **Sect. IV**, we address the problem of better managing a material property database, ***DB-3*** , and estimating its e_3 by briefly describing a PYTHON-based link-up of the two new tools, ANLAP and DATAPLOT-10-Step-Analysis. Again, as described more fully in [52] by Fong and Marcal, the design of a new plug-in named PDA (Python-Dataplot-Anlap) is reported and illustrated with an application to a high temperature mechanical property database for modeling fire-structure interactions. This completes our goal (a) for summarizing the findings of Refs. [50, 51, 52].

In **Sect. V**, we describe the design and implementation of an uncertainty estimation plug-in named PD-UP that has been reported elsewhere by Fong, et al. [49]. We will use extensively this plug-in in subsequent examples involving a probabilistic fracture mechanics (PFM) model, its computational code named PC-PRAISE [17, 27], and the calculation of a quantity named "Cumulative Average Leak Probability (CALP)" over a period of 60 years for a 40.0-cm (15.75-in) diameter, 6.35-cm (2.50-in) wall thickness, 316-NG grade stainless steel pipe hot leg in a water environment with a heat-up-and-cool-down transient event of a maximum temperature surge of 588.56 K (600 F) every 20 years.

In **Sect. VI,** we present the input and output details of a typical Monte-Carlo-based PFM run using PC-PRAISE [17, 27] to calculate CALP, where the distributions of four of the twenty-plus factors identified in the computational model are specified with estimated mean and standard deviation. We adopt the conventional practice of changing one factor at a time to all factors other than those four with distribution parameters to see how the results are affected. Such practice also entails a design of experiment, but the resulting DEX is not orthogonal and has been shown to yield incorrect results (see Ref. [43, p. 312]).

In **Sections VII** through **X,** we describe four case studies where we apply the DEX approach and use PD-UP to conduct a new benchmarking exercise on PC-PRAISE. This exercise allows us to rank the importance of any choice of model parameters suspected of being the major sources of uncertainty [27], and to obtain new estimates of the mean and 95% confidence intervals of CALP that are significantly different from those predicted by PC-PRAISE [17, 27].

A discussion of the significance of our results, some concluding remarks, and a list of references appear in **Sections XI, XII,** and **XIII**, respectively. A truncated version of an output file of a typical PC-PRAISE run with key distributional parameter information is given in **Appendix A**.

II. FAILURE EVENT DATABASE *DB-1*

Failure event reports and their summaries, e.g., a weekly report of the U.S. Department of Energy (DOE) - Office of Nuclear and Facility Safety [14], are usually written in a natural language such as English or Japanese, with data buried in unstructured text. Extraction of information from such text is usually done by engineers to create failure event databases (***DB-1***) for analysis and uncertainty (e_1) estimation. The extraction process is slow, costly, and prone to human errors, which can cause a reduced effectiveness of ***DB-1*** as a critical tool for managing aging structures.

In the first of a series of papers on managing database uncertainties, Marcal, Fong, and Yamagata [50] describes an artificial intelligence (AI) tool named ANLAP [53], which is based on a semantic parsing of a natural language text originally due to Schank [54, 55]. ANLAP is interactive in the sense that a user is first prompted to specify the headings of a table of the extracted information desired by the user. ANLAP is then linked to a public-domain statistical analysis package named DATAPLOT [45] to produce report-quality graphics and data analysis at any level of sophistication.

To illustrate this capability, we show in this paper the results of an exercise based on a 1998 DOE report [14], Section 1 on Spread of Contamination at Hanford (see Figures 4 and 5).

In Figures 6 and 7, we present the printout of ANLAP output files using two DATAPLOT codes named "pedro9.dp" and "pedro9pie.dp." The full text of the specific section of that report is given in [49]. Before linking up with DATAPLOT, the ANLAP output file is a table of two rows of information, namely, a row of headings specified by the user, followed by a second row of data as presented in Figures 6 and 7.

In Figure 8, we add a fictitious set of data for a period prior to that of the real data in order to demonstrate some data analysis capability of the ANLAP-DATAPLOT link, because one needs two rows of data to compute mean and standard deviation). The result is given in Figure 9.

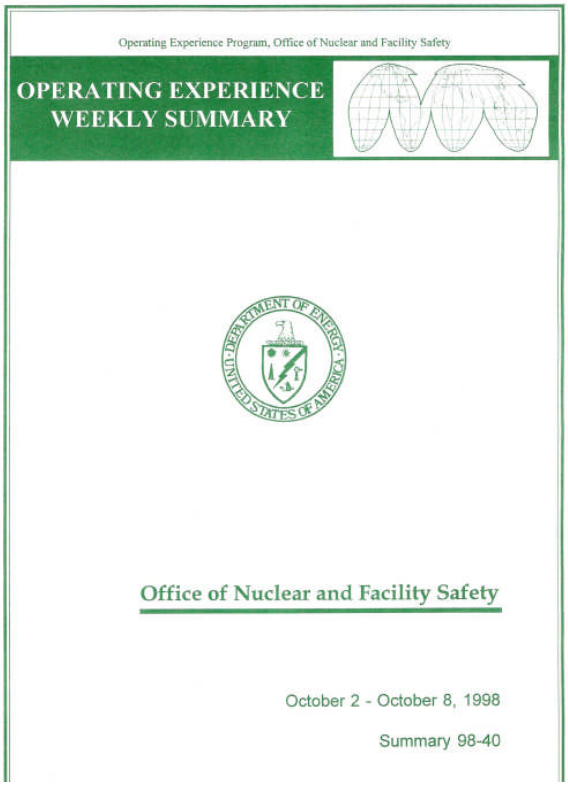

Figure 4. Cover Page of a 1998 DOE weekly report on operating experience of nuclear facilities [14].

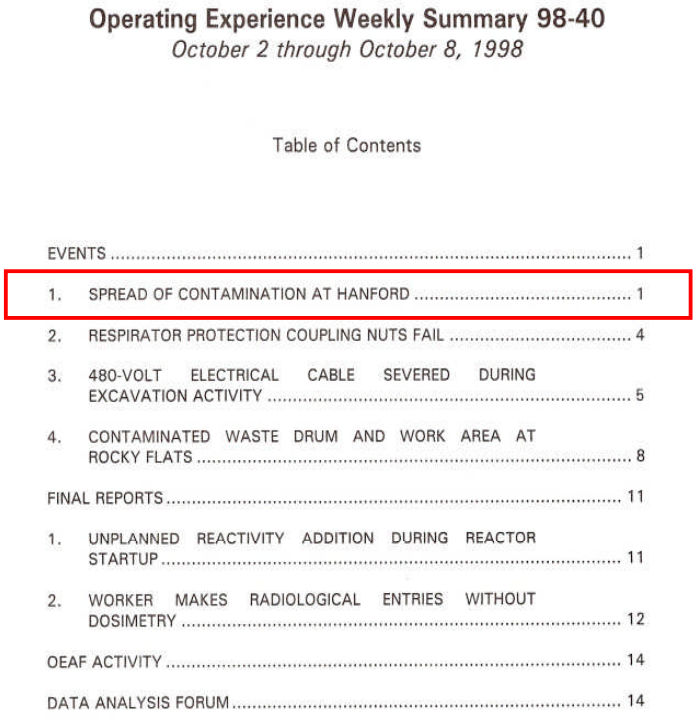

Figure 5. Table of Content Page of a 1998 DOE weekly report on operating experience [14].

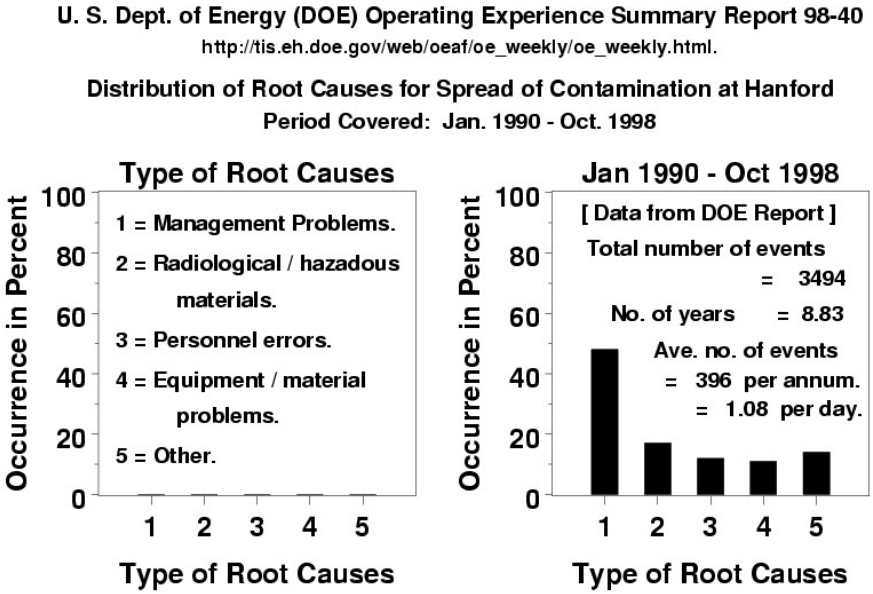

Figure 6. Printout of an ANLAP output file, c:\CD_data\fong201.pdf, using a DATAPLOT code, "pedro9.dp."

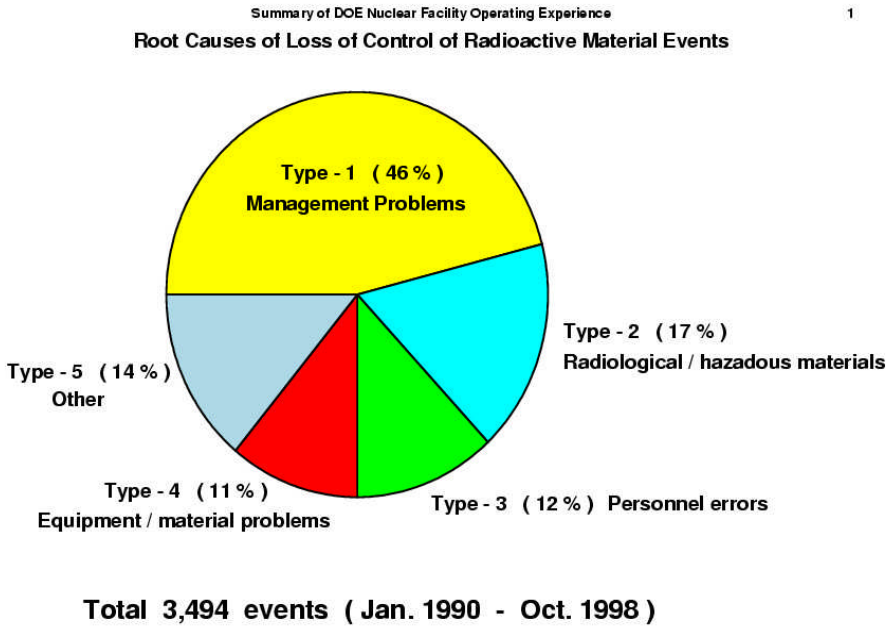

Figure 7. Printout of an ANLAP output file, c:\CD_data\fong202.pdf, using a DATAPLOT code, "pedro9pie.dp."

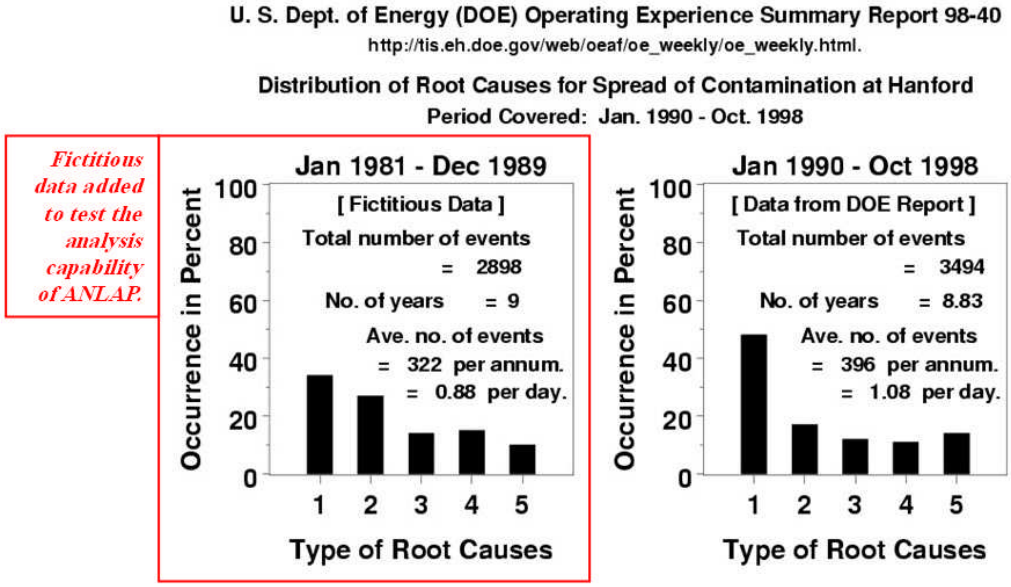

Figure 8. Printout of an ANLAP output file, c:\CD_data\fong203.pdf, using a DATAPLOT code, "pedro10.dp."

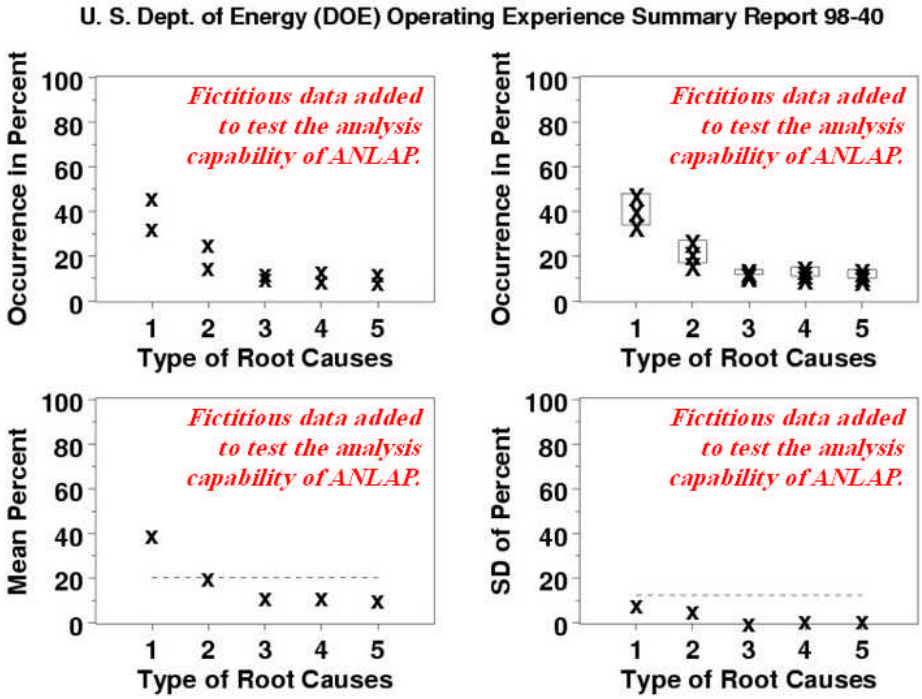

Figure 9. Printout of an ANLAP output file, c:\CD_data\fong204.pdf, using a DATAPLOT code, "pedro11.dp."

III. ISI AND NDE DATABASE *DB-2*

In a 2008 PVP conference paper by Fong, Hedden, Filliben, and Heckert [32], a prototype web-based NDE data analysis methodology to estimate the reliability of weld flaw detection, location, and sizing was described with an example application to the 1968 ultrasonic testing (UT) data of weld seam in PVRC test block 251J and the 1984 sectioning data of the same block implanted with 15 flaws of 4 types.

The methodology was based on the statistical theory of design of experiments (see Box, Hunter, and Hunter [43] and Fong et al [46-49]). A user needs to identify a number of possible factors contributing to the uncertainty of a UT procedure, and to run a few well-designed experiments to rank the relative importance of those factors and find a relationship between the source uncertainties and the result uncertainty.

In that 2008 example [32], five factors were identified as potential contributors of uncertainty to the UT process of Team A in finding an implanted 2-inch crack. They were: (X1) Operator's experience. (X2) UT machine age. (X3) Cable length. (X4) Transducer Probe Angle. (X5) Plastic shoe thickness. As shown in Figures 10 and 11, the resulting analysis using judgment-based fictitious data concluded that the UT operator's experience (X1) and the transducer probe angle (X4) are the two dominant factors contributing to the uncertainty of the Team A's UT results. Again, using the best-judgment-based but fictitious design of experiments (DEX) data, one can rank the relative importance of a large number of factors, identify the two or three dominant ones, and apply a linear least square fit model to estimate the mean and 95% confidence intervals of the crack size as shown in Figure 12.

As a follow-up of that 2008 paper, Fong, Marcal, Hedden, Chao, and Lam [51] extended a recently developed Python-Dataplot Uncertainty Plug-In (PD-UP, see [49]) as a Web-based Uncertainty Plug-In (WUPI) to automate the 2008 methodology such that, for a given NDE database. ***DB-2*** , a user can quickly obtain its uncertainty, e_2 , as one of three types of input to fatigue crack growth models. This specific application to a probabilistic fracture mechanics model is described in Sect. VI.

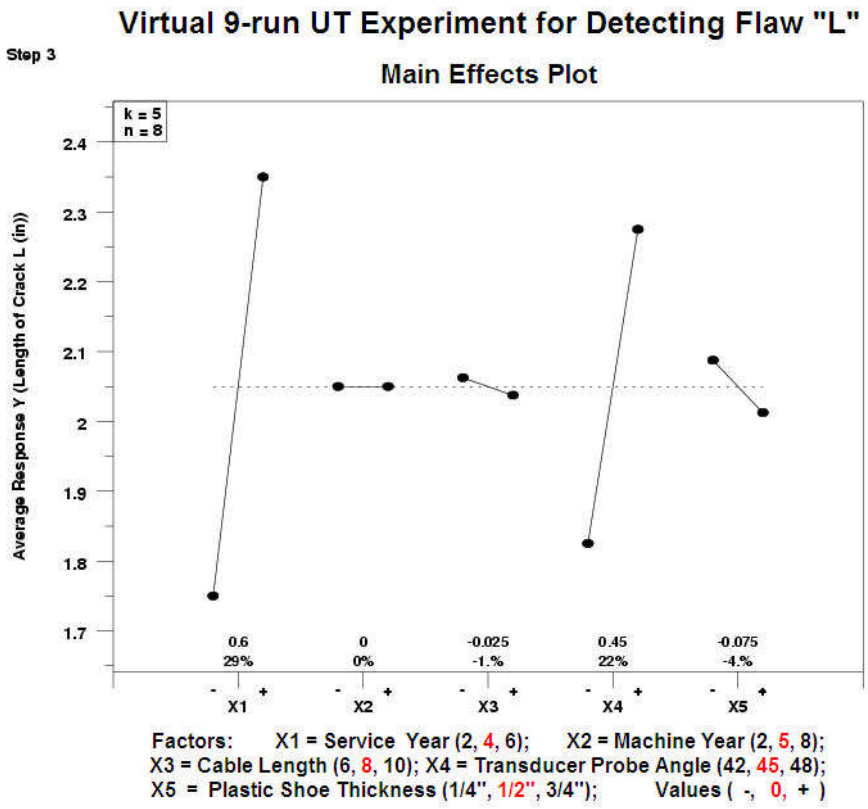

Fig. 10. Step 3 of a 10-step analysis showing the main effects of a 5-factor, 8-run, 2-level fractional factorial design-of-experiments-based exercise (k = 5, n = 8). Note X1 and X4 are dominant (after Fong, et al [32]).

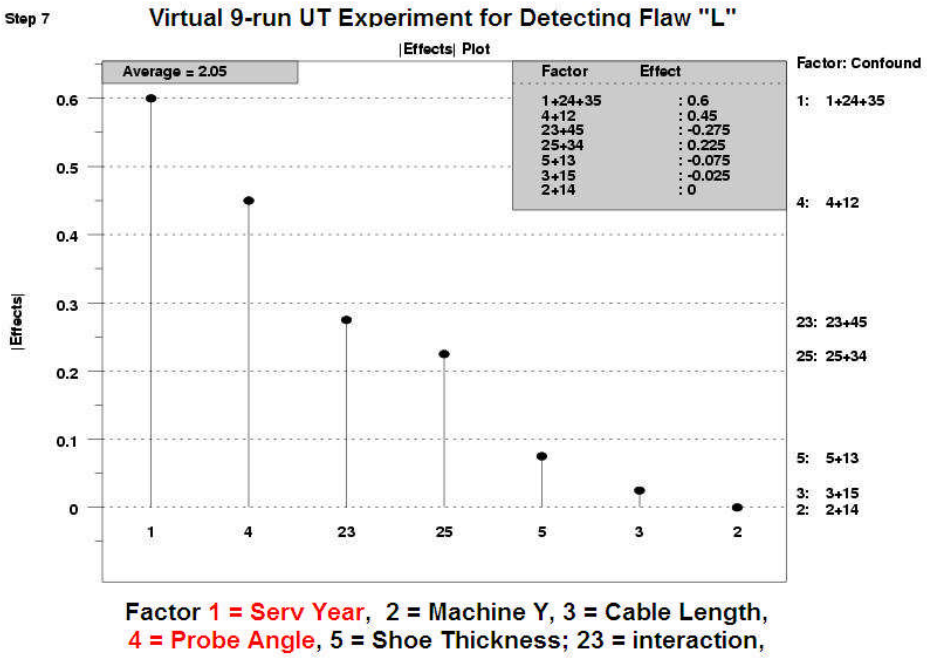

Fig. 11. Step 7 of a 10-step analysis showing the main and interaction effects of a 5-factor, 8-run, 2-level fractional factorial design-of-experiments-based exercise (k = 5, n = 8). Note X1 and X4 are dominant (after Fong,

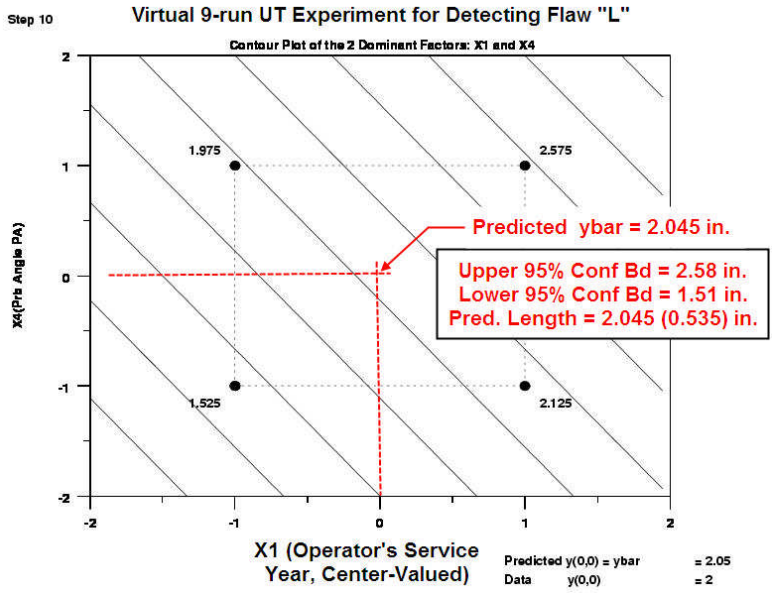

Fig. 12. Step 10 of a 10-step analysis showing a contour plot of the two dominant factors, X1, and X4. The plane behavior of the plot confirms that the 2-term interactions are negligible. The two-parameter least square fit model gives an estimated crack size with 95% confidence half-interval as 2.045 (0.535) in. (after Fong, et al [32]).

IV. MATERIAL PROPERTY DATABASE *DB-3*

As mentioned in Sect. I, material property databases, ***DB-3***, contain both global and local information, and it is essential to report with care its uncertainty, e_3 . By and large, most ***DB-3's*** are global, and there is a long history of research in computer-assisted ***DB-3*** dating back to the early 1970s with advances in structural English query languages [56-58] and to the early 1980s with the arrival of PC's and expert systems [59-66].

Again drawing on the medical analogy of distinguishing health statistics databases (global) that set the "normal" ranges of a healthy person, from the historical data of a patient's blood chemistry, etc. (local), engineers need to know how to interpret uncertainty e_3 of a global ***DB-3*** in the context of a "usable" uncertainty of a local one, when such input is needed for predictive fatigue life models such as PC-PRAISE. To illustrate this point, we offer three examples from recent papers [33, 68, 69] and a new tool in the third of this 4-paper series by Fong and Marcal [52] as detailed below:

4.1. In a global ***DB-3*** reported by Gerberich and Moody [70] and discussed by Fong, Ranson, Vachon, and Marcal [33], a strong variation of the crack growth law exponent m with test temperature for iron and various steels at R-ratios near zero is shown in Figure 13. Note the spread of m at 300 K is about a factor of two.

4.2. In a local ***DB-3*** reported by Interrante and Hicho [67] and benchmarked by Interrante, Fong, Filliben, and Heckert [68], a strong variation of the Charpy V-notch energy with test temperature for an ASTM A517 Grade H steel plate is shown in Fig. 14. That in turn caused a strong variation of the estimated static crack initiation toughness value as shown in Fig. 15.

4.3. In a local ***DB-3*** reported by Sherry, Lidbury, and Beardmore [72] and benchmarked by Chao, Fong, and Lam [69], a global uncertainty e_3 estimated for the static crack initiation toughness, as shown in Fig. 16, takes the value of 13.68 as the 95% confidence half-interval, whereas the local e_3 estimated by a tolerance-interval-based approach [69] for a 99% coverage and 95% confidence takes the value of 23.10, which is about 70% higher than the global one.

4.4. The extrapolation of e_3 in a global ***DB-3*** to a local one is automated by Fong and Marcal [52] in the design of a Dataplot-Python-Anlap (DPA) plug-in with an application in modeling fire-structure interactions using a high-temperature mechanical property database created by NRIM in Japan [73].

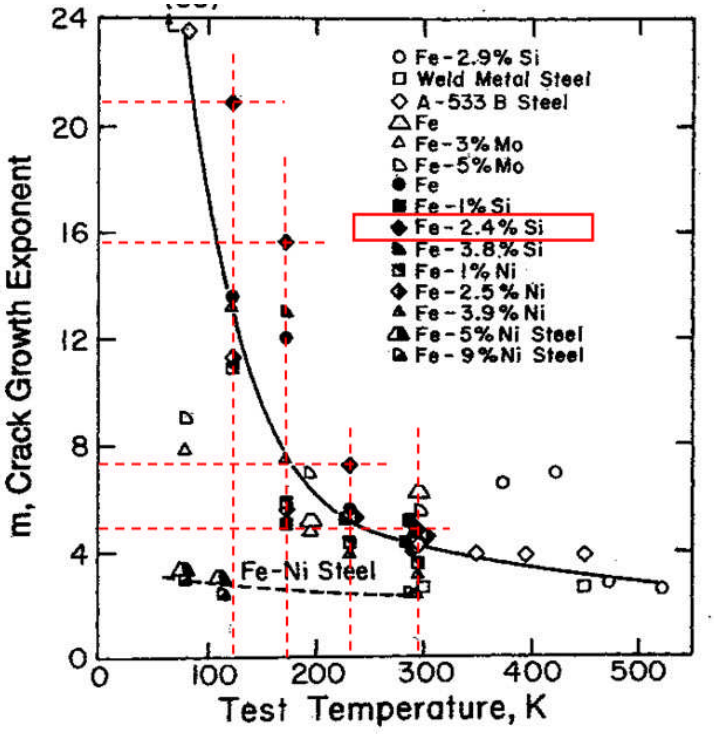

Fig. 13. Variation of the exponent m with test temperature for iron and various steels at R-ratios near zero (after Gerberich and Moody [70]). Note that for Fe-2.4%Si (solid diamond), the spread of m is wide, ranging from 21 at 120 K to 5 at 293 K. After Fong, Ranson, Vachon, and Marcal [33].

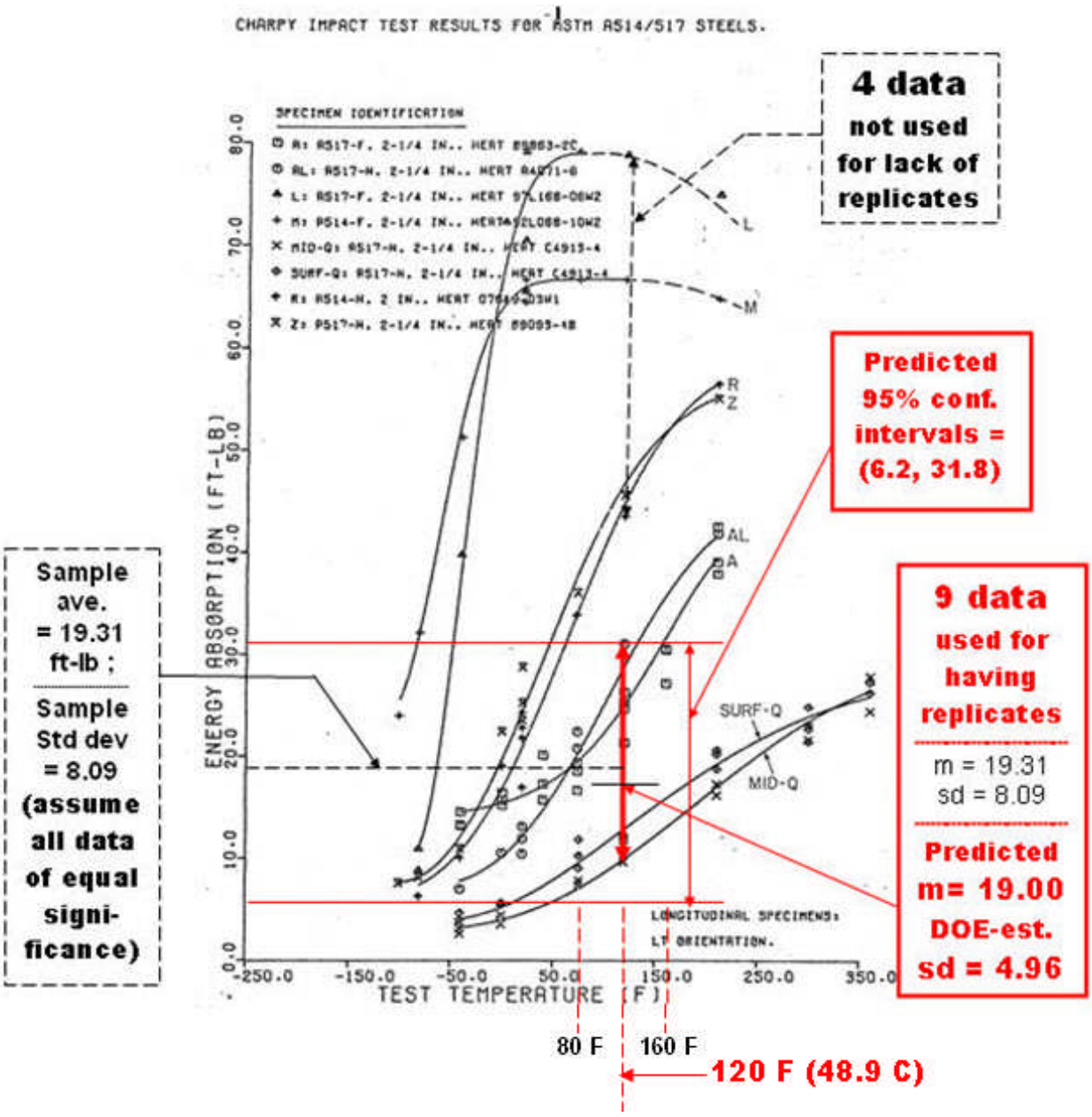

Fig. 14. Comparison of an estimated Charpy V-notch energy at 120 °F (48.9 °C) based on a DEX-generated *fictitious* data set for an ASTM A517 Grade H steel plate (620 MPa min. room temperature yield strength), with the same experimental data reported by Interrante and Hicho [67] in 1973. After Interrante, Fong, Filliben and Heckert [68].

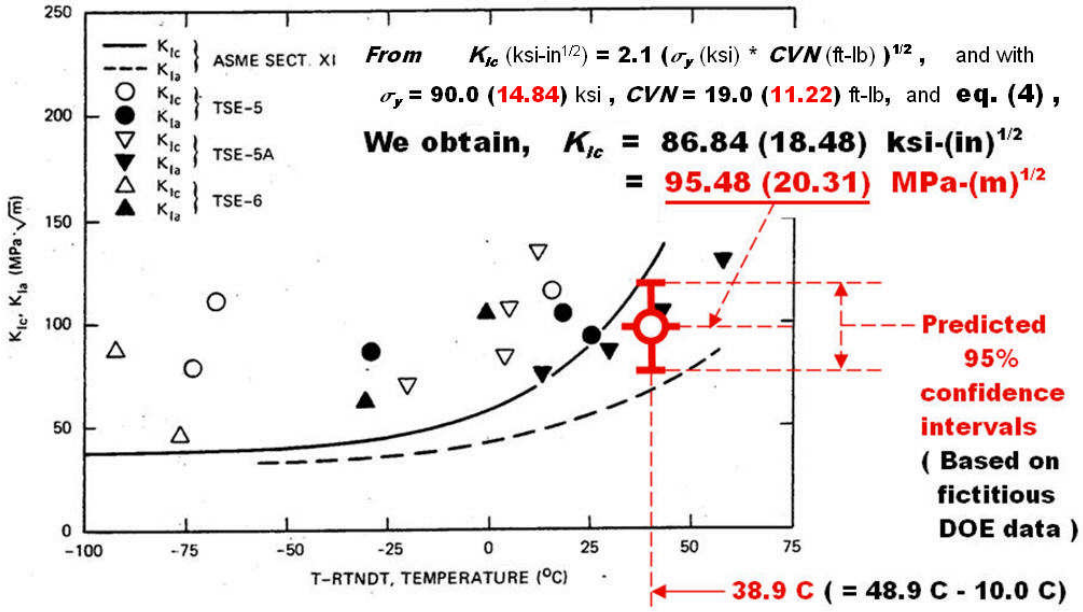

Fig. 15. Plot of an estimated static crack initiation toughness (K_{Ic}) value with an expression of uncertainty (error bar in red) based on *fictitious* design-of-experiments-generated results at 120 °F (48.9 °C), in a *K* vs. (*T* - RTNDT) diagram where K_{Ic} and K_{Ia} data from three thermal shock experiment (TSE) test cylinders, TSE-5, 5A, and 6, and ASME Section XI K_{Ic} and K_{Ia} curves over a broad range of temperature shift, (*T* - RTNDT), were plotted by Cheverton et al [71]. Note that all experimental data or design curves are for comparable steels having an room temperature yield strength of about 90 ksi (620.6 MPa). After Interrante, Fong, Filliben and

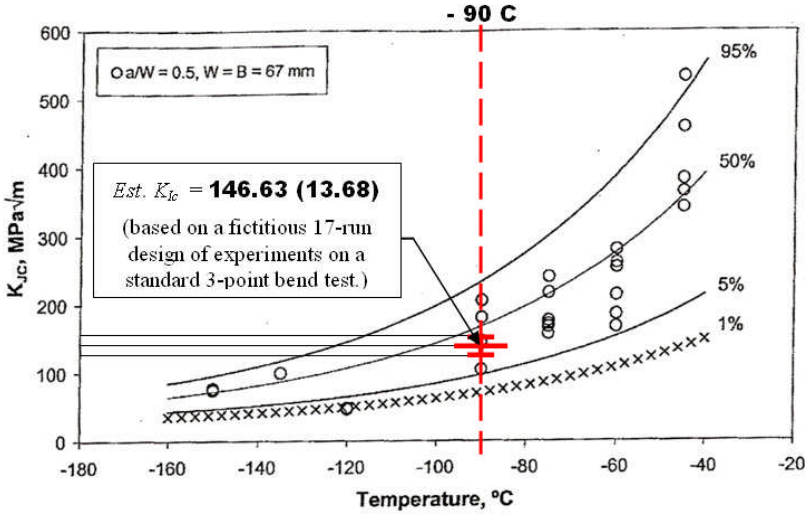

Fig. 16. Comparison of the estimated mean and standard deviation of K_{Ic} at -90 C based on a 8-factor, 17-run DOE-generated *fictitious* test data for ASTM A533 Grade B-1 steel plate (580.6 MPa yield strength at -90 C), with K_{Ic} data of a validation experiment using same grade of steels of comparable yield strength (see Sherry, Lidbury, and Beardmore [72]). After Chao, Fong, and Lam [69].

V. A PYTHON-DATAPLOT UNCERTAINTY PLUG-IN

Before introducing an uncertainty estimation plug-in, we offer a a brief introduction of the theory of Design of EXperiments (DEX) and the 10-step DATAPLOT-based analysis [45] to readers unfamiliar with those tools. Those familiar with them may wish to skip and go directly to a description of PD-UP.

5.1 What is DEX ?

Ans. Given a model with well defined input variables, parameters, and response variables, we conduct a virtual experiment by changing one or more physical process variables (to be called factors) in order to observe the effect the changes have on one or more response variables. A design of such virtual experiment (DEX) begins with determining the *objectives* of such experiment and selecting the *process factors* for the study. An experimental design is the laying out of a detailed experimental plan in advance of doing the experiment. The statistical theory underlying DEX begins with the concept of *process models*. A process *model* of the 'black box' type is formulated with several discrete or continuous input *factors* that can be controlled, and one or more measured output *responses*. The output responses are assumed continuous. Real or virtual experimental data are used to derive an empirical (approximate) model linking the outputs and inputs. These empirical models generally contain *first-order (linear) and second-order (quadratic and interactions) terms.*

5.2 What is a first order model ?

Ans. A first-order model with only three factors, X_1, X_2 and X_3, can be written as

$$Y= \beta_0+\beta_1X_1+\beta_2X_2+\beta_3X_3+\beta_{12}X_1X_2+\beta_{13}X_1X_3+\beta_{23}X_2X_3 + errors \quad (2)$$

Here, Y is the response for given levels of the main effects X_1, X_2 and X_3, and the X_1X_2 , X_1X_3 , X_2X_3 terms are included to account for a possible interaction effect between X_1 and X_2 , X_1 and X_3 , X_2 and X_3 , respectively. The constant β_0 is the response of Y when both main effects are 0. In one of the examples that follows, we use a linear model with five factors and one response variable, and the total number of terms on the right hand side of eq. (2) is 2^5 , or 32.

5.3 How does one selecte factors and responses ?

Ans. Process variables of an experiment include both inputs (factors) and outputs (responses). The selection criteria are:

(a) Include all important factors (based on judgment).
(b) Be bold in choosing the low and high factor levels.
(c) Check the factor settings for impractical or impossible com-binations, such as very low pressure or very high gas flows.
(d) Include all relevant responses.
(e) Avoid using only responses that combine two or more measurements of the process. For example, if interested in the ratio of two rates, measure both rates, not just the ratio.

We have to choose the range of the settings for input factors, and it is wise to give this some thought beforehand rather than just try extreme values.

5.4 How does one select an experimental design?

Ans. The most popular experimental designs are *two-level designs*. Why only two levels? There are a number of good reasons why two is the most common choice amongst engineers; one reason is that it is ideal for screening designs, simple and economical; it also gives most of the information required to go to a multilevel response surface experiment if one is needed. The standard layout for a 2-level design uses +1 and -1 notation to denote the "high level" and the "low level" respectively, for each factor. For example, the matrix below

	Factor 1 (X1)	Factor 2 (X2)
Trial 1	- 1	- 1
Trial 2	+1	- 1
Trial 3	- 1	+1
Trial 4	+1	+1

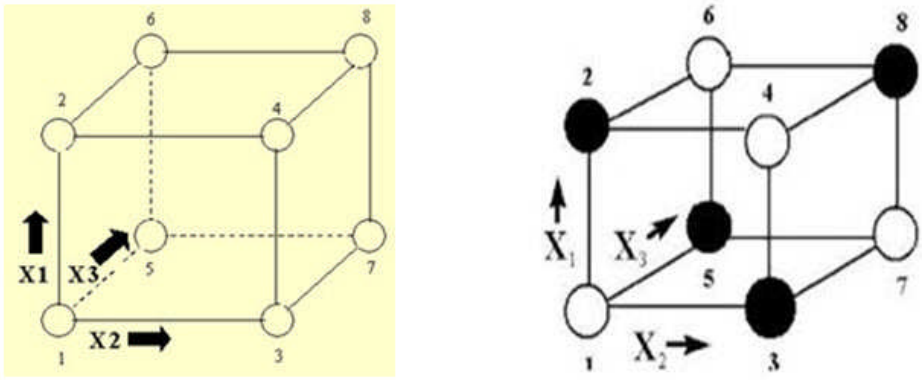

Fig. 17. (left) A full-factorial 8-run orthogonal design for 3 factors. (right) A fractional factorial 4-run orthogonal design for 3 factors.

describes an experiment in which 4 trials (or runs) were conducted with each factor set to high or low during a run according to whether the matrix had a +1 or -1 set for the factor during that trial. If the experiment had more than 2 factors, there would be an additional column in the matrix for each additional factor. For example, a 3-factor full factorial design is represented by the following matrix:

Order of Run	X1	X2	X3
1	- 1	- 1	- 1
2	+1	- 1	- 1
3	- 1	+1	- 1
4	+1	+1	- 1
5	- 1	- 1	+1
6	+1	- 1	+1
7	- 1	+1	+1
8	+1	+1	+1

5.5 What is a 2-level full factorial DEX?

Ans. A common experimental design is one with all input factors set at two levels each. These levels are called 'high' and 'low', or '+1' and '-1', respectively. A design with all possible high/low combinations of all the input factors is called a full factorial design of experiments in two levels. If there are k factors, each at 2 levels, a full factorial DEX has 2^k runs. Fig. 17 (left) is a graphical representation of a 2-level, 3-factor, 2^3 or 8-run full factorial DEX. This implies eight runs (not counting replications or center point runs). The arrows show the direction of increase of the factors. The numbers '1' through '8' at the corners of the design box reference the "Standard Order" of runs (also referred to as the "Yates Order", see Croarkin, et al [51]). When the number of factors is 5 or greater, a full factorial DEX requires a large number of runs and is not very efficient. This is where a need for a fractional factorial DEX comes in.

5.6 What is a Center Point in a 2-level design?

Ans. To introduce the concept of a center point, we again refer to Fig. 17 (left), a graphical representation of a two-level, full factorial design for three factors, namely, the 2^3 design. As mentioned earlier, we adopt the convention of +1 and -1 for the factor settings of a two-level design. When we include a center point during the experiment, we mean a point located in the middle of the design cube, and the convention is to denote a center point by the value "0".

5.7 What is a 2-level fractional factorial DEX?

Ans. A fractional factorial DEX is a factorial experiment in which only an adequately chosen fraction of the treatment combinations required for the complete factorial experiment is selected to be run. In general, we pick a fraction such as ½, ¼, etc. of the runs called for by the full factorial. We use various strategies that ensure an appropriate choice of runs. Properly chosen fractional factorial designs for 2-level experiments have the desirable properties of being both *balanced* and *orthogonal.* For example, the following matrix represents a 3-factor half-factorial design:

Order of Run	X1	X2	X3 (X1*X2)
1 (new), 5 (old)	- 1	- 1	+1
2 (new), 2 (old)	+1	- 1	- 1
3 (new), 3 (old)	- 1	+1	- 1
4 (new), 8 (old)	+1	+1	+1

A comparison of the half-fractional factorial design, as shown in Fig. 17 (right), with that of the full factorial design shown in Fig. 17 (left), reveals the balanced and orthogonal nature of the DEX concept.

5.8 What is a 10-step DEX-based Exploratory Data Analysis ?

Ans. Let us introduce the so-called Exploratory Data Analysis (EDA_ approach of DATAPLOT to a screening problem in experimental design and its 10-step algorithm. In general, there are two characteristics of a screening problem: (a) There are many factors to consider. (b) Each of these factors may be either continuous or discrete. The desired output from the analysis of a screening problem is:

1. A ranked list (by order of importance) of factors.
2. The best settings for each of the factors.
3. A good model.
4. Insight.

The essentials of the screen problem are:

1. There are k factors with n observations.
2. The generic model is

$$Y = f(X_1, X_2, ..., X_k) \qquad (3)$$

In particular, the EDA approach implemented in DATAPLOT is applied to 2^k full factorial and 2^{k-p} fractional factorial designs. Let us introduce a 10-step EDA process for analyzing the data from 2^k full factorial and 2^{k-p} fractional factorial designs as follows:

Step 1. Ordered data plot.
Step 2. DEX scatter plot.
Step 3. DEX mean plot.
Step 4. Interaction effects matrix plot.
Step 5. Block plot.
Step 6. DEX Youden plot.
Step 7. |Effects| plot.
Step 8. Half-normal probability plot.
Step 9. Cumulative residual standard deviation plot.
Step 10. DEX contour plot of two dominant factors.

Each of these plots will be presented with the following format:

1. Purpose of the plot. 2. Output of the plot.
3. Definition of the plot. 4. Motivation for the plot.
5. An example of the plot. 6. An interpretation of the plot.
7. Conclusions we can draw from the plots. [THE END].

V. A PYTHON-DP UNCERTAINTY PLUG-IN (CONT'D)

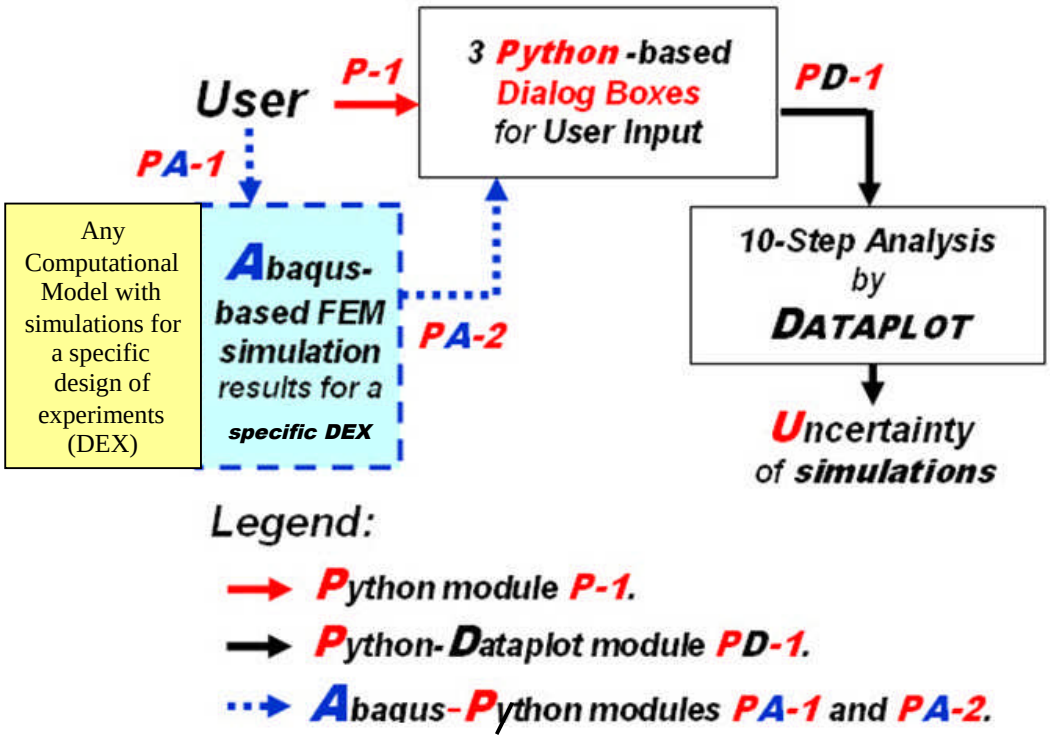

Fig. 18. A Conceptual Design of the Python-Dataplot-Uncertainty Plug-In.

In Fig. 18, we show a conceptual design of a DEX-based uncertainty plug-in, PD-UP, where a user is required to have access to a well-defined computational model such as an ABAQUS input file [46] or a Fortran code named PC-PRAISE [17]. In addition, the user is required to have identified k number of factors, $X1, X2, \ldots, Xk$, with a known set of base values that defines the center point of a 2-level DEX.

As shown in Fig. 19, the user is prompted by Button_1 of PD-UP (v. 1.0) to answer a few questions on the nature of the k factors and their individual percentage variations. All factors are assumed to be continuous variables in the first version of PD-UP. Discrete variables will be allowed in a future version of the plug-in. A typical output file created by PD-UP for a 3-factor, 2-level design is given in Fig. 20. Button_1 is also known as the *k*-button, because it requires a user's input of k.

The second button, also known as the *n*-button or Button_2, provides the user with a choice of either a full factorial DEX, in which case, $n = 2^k$, or a number of fractional factorial DEX, with n ranging from 2^{k-1}, down to 2^{k-2}, etc. until n reaches its lowest possible number that must be at least one greater than k.

.

Once the user specifies a value of k in Button_1 (Fig. 19) and a value of n in Button_2 (Fig. 21), an orthogonal DEX, either a full or a fractional factorial one, is created by PD-UP. This is followed by n number of computer runs plus a center point, either automatically by a PD-UP adjunct utility code or manually by the user. The results of the $n+1$ computer runs are stored in a file created by Button_2, as shown in Fig. 22 for a 3-factor, 9-run, 2-level DEX.

The third button, also known as the review and 10-step button (Button_3), provides the user an opportunity to verify the intended values of k, n, base values of k factors, percentage variations of the k factors, names and symbols of the k factors, and the name, symbol, and $n+1$ values of the result variable. This is shown in Fig. 20. The lower left window entitled "DOE Table for review" uses DOE as an alternative acronym for DEX, a practice we have discontinued to avoid a confusion with the official acronym of the U.S. Department of Energy.

After the user approves the three windows, a 10-step analysis of the DEX-based result data is carried out using a DATAPLOT code named "pedro7.dp." More details appear in Ref. [46].

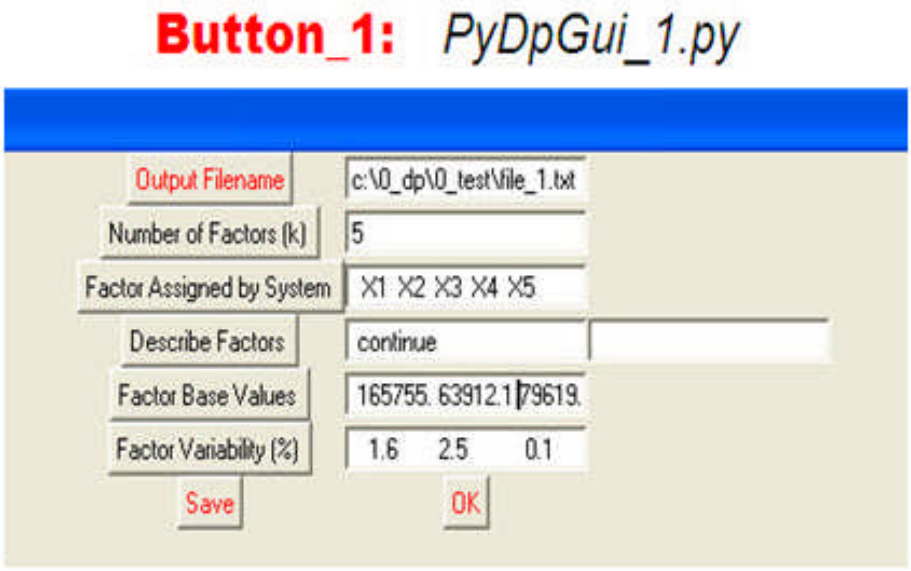

Fig. 19. Button_1 to define *k* factors and enter their variability

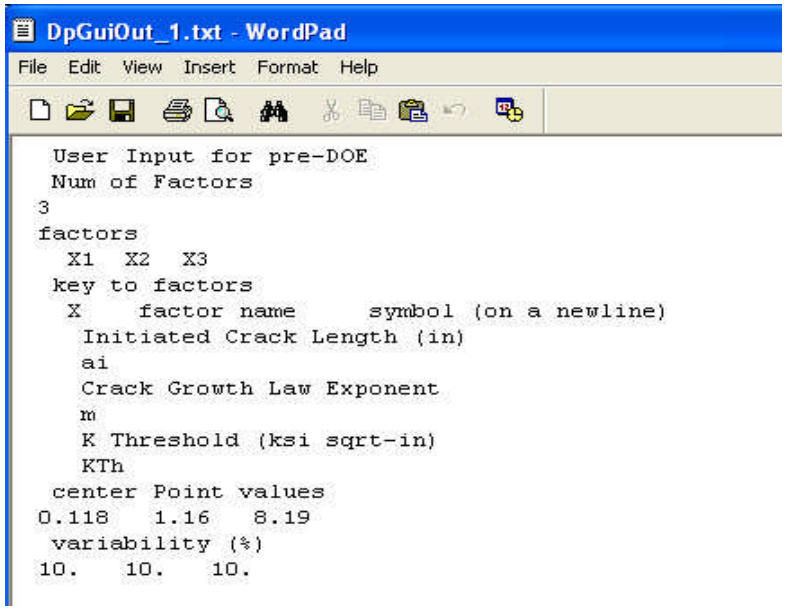

Fig. 20. A PD-UP Button_1 output file named DpGuiOut_1.txt created for a 3-Factor PC-PRAISE DEX-1 Run.

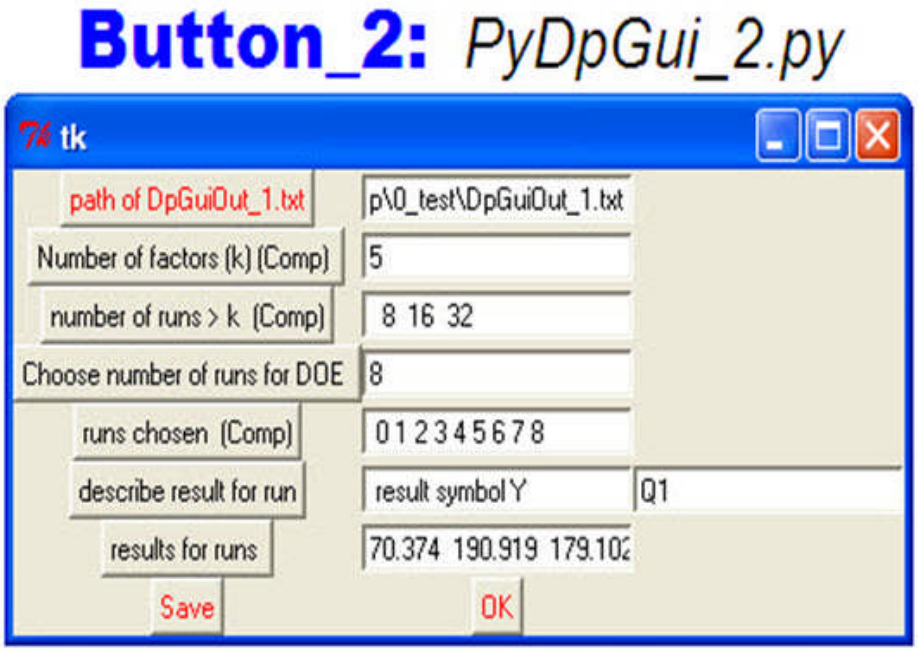

Fig. 21. Button_2 to choose *n* runs for a (*k, n*) design and enter results.

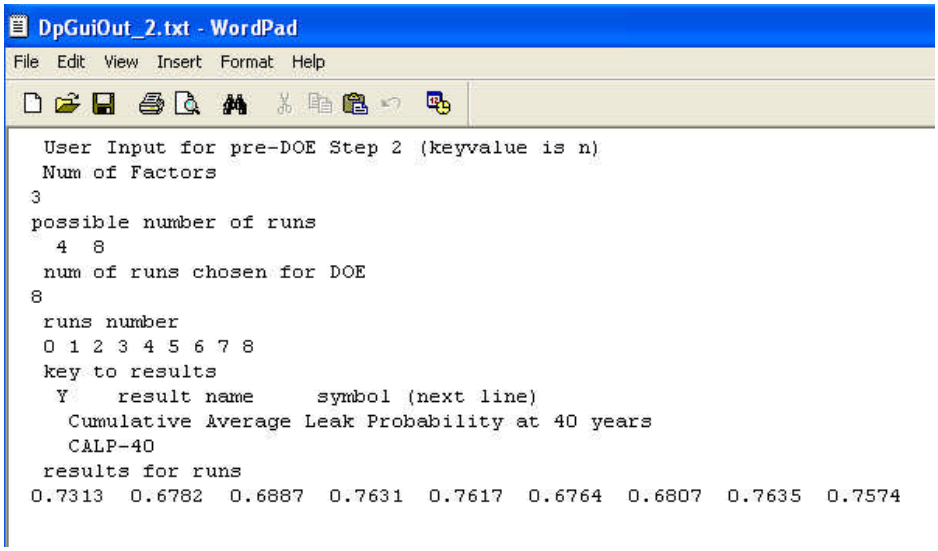

Fig. 22. A PD-UP Button_2 output file named DpGuiOut_2.txt created for a 3-Factor, 8-RUN+Center-Point PC-PRAISE DEX-1 Simulation Run for Estimating Mean and Confidence Intervals of CALP-40.

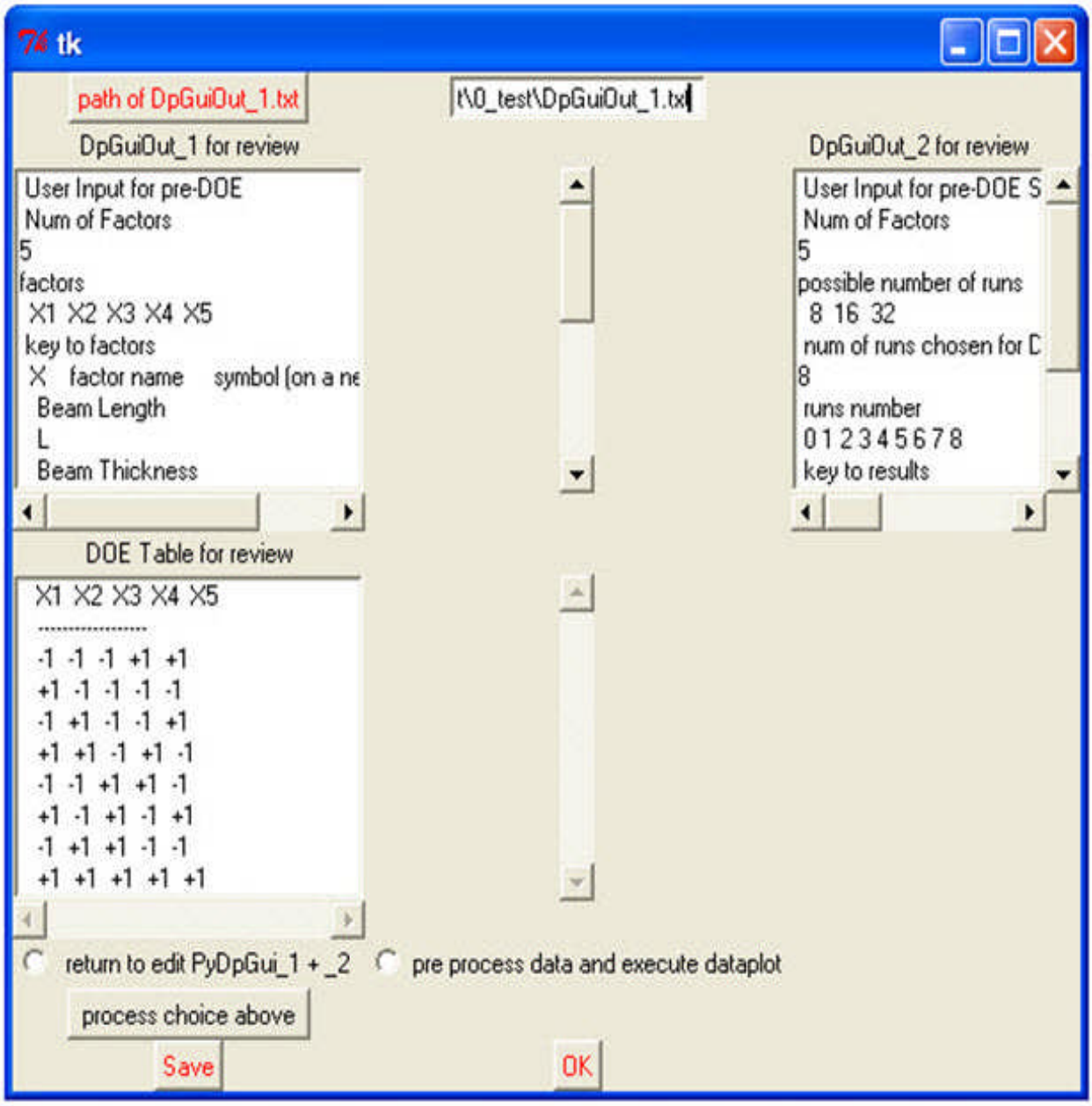

Fig. 23. Button_3 with two of three output screens.

VI. A TYPICAL PIPE LEAK PROBABILITY MODEL

In a 2000 landmark study by Khaleel, Simonen, Phan, Harris, and Dedhia [17] entitled "Fatigue Analysis of Components for 60-Year Plant Life," the authors compared through-wall crack (TWC) frequencies at the end of a 40-year plant life to those at the end of a 60-year plant life, and component-failure probabilities for a reactor water environment with those for an air environment. The authors concluded from their computer models using a Fortran code named PC-PRAISE [17] that

". . .the critical components with the highest probabilities of failure can have through-wall crack frequencies that are on the order of about $5x10^{-2}$ per year. However, these components show little or no increase in the failure frequency from 40 years to 60 years.

" ... Calculated core-damage frequencies for the components with the highest failure frequencies show essentially no increase in core-damage frequency from 40 to 60 years."

At a time when nuclear plant operators were requesting license renewal for extending the permissible plant life from 40 to 60 years [40], those conclusions were most reassuring.

However, Simonen, Gosselin, Lydell, Rudland, and Wikowski [27] in a 2007 computer model benchmarking study reported significant differences between the model-predicted probabilities and those derived from field data (***DB-1***) in three pressurized water reactor (PWR) and one boiling water reactor (BWR) cases by factors ranging from 30 to 10,000.

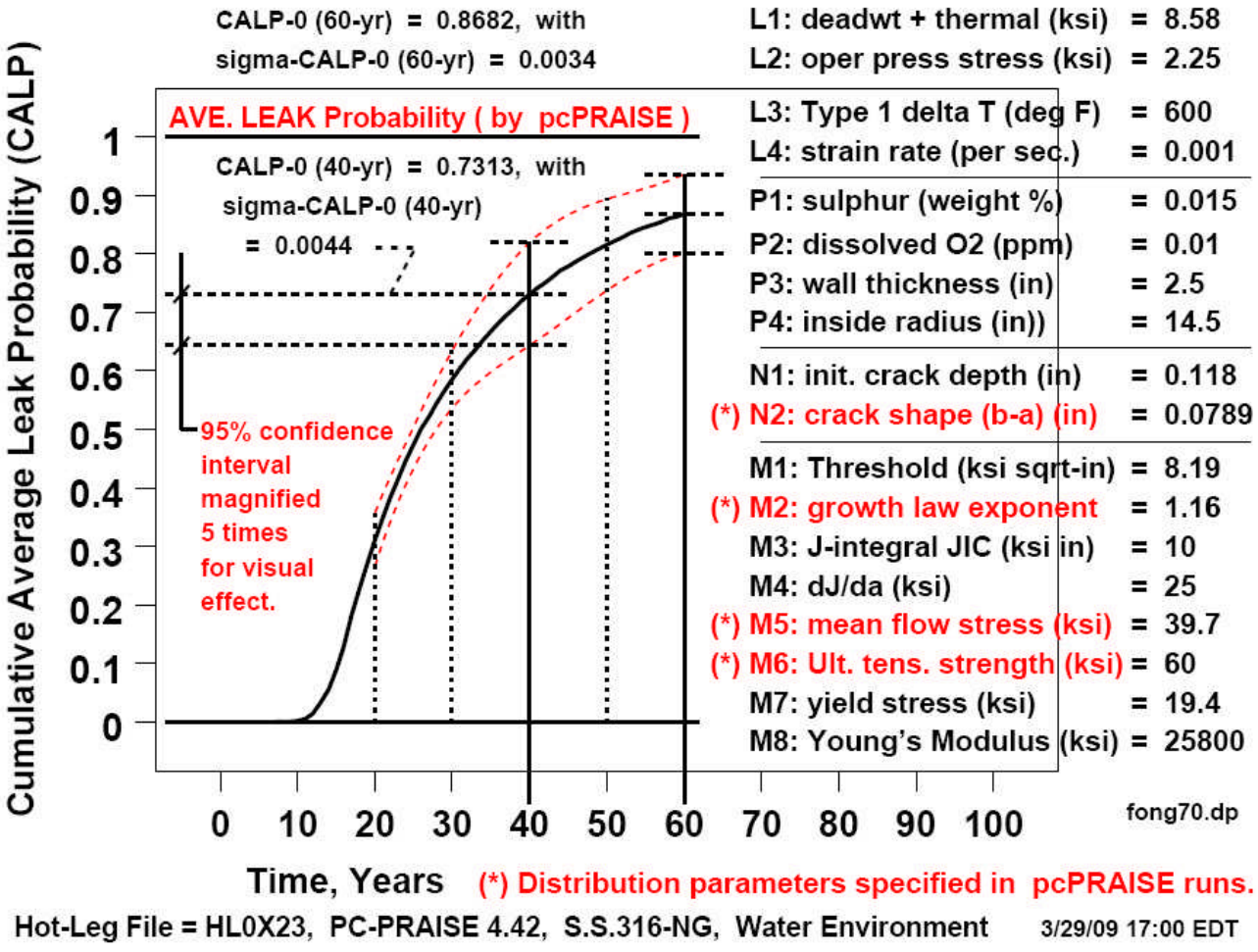

Fig. 24. A plot of the cumulative average leak probability (CALP) versus time based on the output file of a PC-PRAISE (v. 4.42) run using 4 distributional parameters (red) and 20+ constants as shown in Table 2. Table 2 also lists a history of the standard deviation, σ, of CALP, which is quite small and requires magnification for visuals.

VI. A TYPICAL CALP RUN USING PRAISE (CONT'D)

Table 2. PIPING RELIABILITY ANALYSIS INCLUDING SEISMIC EVENTS (PRAISE)
PC-PRAISE VERSION 4.42
EXECUTED ON 03/17/2009 AT 8:53p
ECHO-PRINT OF INPUT DATA IN FILE X230.DAT

```
    1>HOT-LEG FILE=HL0X23  PROB-CALC  SIM=10^4   90 CRKS
    2>    3    0   90   -4         0     1.100         0   14    688    72
    3> -100    1    2    0 -0.2    0    0    0     0    0    0    0    0    0    0    0    0
    4>         0      .015      0.01     0.118    0.0789    0.0001    0    0       1.0
    5>      60.0  .200E+00    0    0
    6>     2.500      14.50      10.0
    7>      8.19       1.16 6.327E-07 1.141E-06       1.0
    8> .3970E+02 .3970E+01       10 0      25.0      19.4     106.0   25800.0      5.00
    9>      60.0        6.0    0
   10>  .100E+01  .500E+02                          -3.50     -1.20
   11>      2.08      8.58     2.250     -3.00  .100E+01  .000E+00
   12>    6    9  100  100
   13>      .010      .100      .200      .300      .400      .500      .600      .700
   14>      .800
   15>     1.000     2.000     3.000     4.000     5.000     6.000
   16>    1      20.0 600. HEAT-UP AND COOL-DOWN
   17>   .001000          1
   18> 1000    .00008 590. # 1  HIGH-STR/LOW-CYCLE  SEE NOTES BELOW 500000 CYCLES/40 Y
                          37.790
```

N2: crack shape ellipticity (b-a)

M2: crack growth law exponent (m)

M5: mean flow stress

M6: Ultimate tensile

Cumulative Average Leak Probability (CALP)

```
                                                LEAK DETECTION AND DEFINITION PARAMETERS
                                                DETECTABLE LEAK (GPM) =    1.00
                                                BIG LEAK        (GPM) =   50.00
- - - HOT-LEG FILE=HL0X23  PROB-CALC  SIM=10^4   90 CRKS - - -
                            - - - RESULTS WITHOUT EARTHQUAKES - - -
          SEISMIC CLASS INFORMATION
                             CLASS     SIGEQ      SGLCEQ    CYCLES  COV F-BM
                               0     .0000E+00      .000       0       .0000
          PROBABILITY OF FAILURE FOR UNCRACKED PIPE AND INTERPOLATED VALUES
```

Sigma Leak (leak-σ)

TIME	AVG LEAK	AVG BIG LEAK	AVG LOCA	SIGMA LEAK	SIGMA BIG LEAK	SIGMA LOCA
.000	0.00000E+00	0.00000E+00	0.00000E+00	0.00000E+00	0.00000E+00	0.00000E+00
2.000	0.00000E+00	0.00000E+00	0.00000E+00	0.00000E+00	0.00000E+00	0.00000E+00
4.000	0.00000E+00	0.00000E+00	0.00000E+00	0.00000E+00	0.00000E+00	0.00000E+00
6.000	1.00000E-04	0.00000E+00	0.00000E+00	1.00000E-04	0.00000E+00	0.00000E+00
8.000	4.00000E-04	0.00000E+00	0.00000E+00	1.99970E-04	0.00000E+00	0.00000E+00
10.000	2.40000E-03	1.10000E-03	0.00000E+00	4.89334E-04	3.31497E-04	0.00000E+00
12.000	1.49000E-02	9.10000E-03	0.00000E+00	1.21159E-03	9.49636E-04	0.00000E+00
14.000	5.52000E-02	4.08000E-02	0.00000E+00	2.28382E-03	1.97836E-03	0.00000E+00
16.000	1.29000E-01	1.02500E-01	1.00000E-04	3.35217E-03	3.03320E-03	1.00000E-04
18.000	2.27500E-01	1.86600E-01	1.00000E-03	4.19239E-03	3.89610E-03	3.16085E-04
20.000	3.11800E-01	2.54600E-01	2.20000E-03	4.63252E-03	4.35658E-03	4.68549E-04
22.000	3.83700E-01	3.09000E-01	2.60000E-03	4.86311E-03	4.62104E-03	5.09264E-04
24.000	4.47400E-01	3.56700E-01	2.80000E-03	4.97250E-03	4.79049E-03	5.28435E-04
26.000	5.01100E-01	3.92900E-01	2.90000E-03	5.00024E-03	4.88419E-03	5.37762E-04
28.000	5.45800E-01	4.21900E-01	3.00000E-03	4.97923E-03	4.93887E-03	5.46928E-04
30.000	5.85600E-01	4.46000E-01	3.00000E-03	4.92643E-03	4.97100E-03	5.46928E-04
32.000	6.22000E-01	4.68100E-01	3.00000E-03	4.84912E-03	4.99006E-03	5.46928E-04
34.000	6.53300E-01	4.85000E-01	3.00000E-03	4.75943E-03	4.99800E-03	5.46928E-04
36.000	6.82200E-01	4.99300E-01	3.00000E-03	4.65645E-03	5.00025E-03	5.46928E-04
38.000	7.07500E-01	5.10900E-01	3.00000E-03	4.54933E-03	4.99906E-03	5.46928E-04
40.000	7.31300E-01	5.22600E-01	3.00000E-03	4.43306E-03	4.99514E-03	5.46928E-04
42.000	7.50600E-01	5.31800E-01	3.00000E-03	4.32687E-03	4.99013E-03	5.46928E-04
44.000	7.71900E-01	5.39300E-01	3.00000E-03	4.19628E-03	4.98478E-03	5.46928E-04
46.000	7.87300E-01	5.45700E-01	3.00000E-03	4.09238E-03	4.97932E-03	5.46928E-04
48.000	8.02100E-01	5.50800E-01	3.00000E-03	3.98436E-03	4.97438E-03	5.46928E-04
50.000	8.15500E-01	5.56600E-01	3.00000E-03	3.87911E-03	4.96811E-03	5.46928E-04
52.000	8.28600E-01	5.61600E-01	3.00000E-03	3.76877E-03	4.96216E-03	5.46928E-04
54.000	8.41100E-01	5.65400E-01	3.00000E-03	3.65601E-03	4.95729E-03	5.46928E-04
56.000	8.50000E-01	5.68200E-01	3.00000E-03	3.57089E-03	4.95352E-03	5.46928E-04
58.000	8.60500E-01	5.71200E-01	3.00000E-03	3.46485E-03	4.94929E-03	5.46928E-04
60.000	8.68200E-01	5.73800E-01	3.00000E-03	3.38290E-03	4.94548E-03	5.46928E-04

VI. A TYPICAL CALP RUN USING PRAISE (CONT'D)

In Fig. 24, we show a plot of the cumulative average leak probability (CALP) of a 316-NG stainless steel pipe hot log vs. time based on the output file of a PC-PRAISE run using 4 distributional parameters, **N2, M2, M5, M6** , with values given in Table 2. We also plot the 2σ confidence intervals, magnified 5 times for visual effects, using the leak-σ data also listed in Table 2.

In computing failure probabilities including CALP, the authors of PC-PRAISE assumed the crack propagation to start from a 3-mm (0.118-in) deep initiated flaw, and stated in their 2000 report [17, p.3.2] ". . . not to include the initial crack depth as a variable to be simulated by the probabilistic model." Many NDE studies including ours [10, 11, 20, 21, 24, 28, 32, 33] showed the uncertainty in the size of a detected crack to be somewhat large, so we decided to run the same PC-PRAISE code with a simple, straight 20% increase in **N1**, the initial crack depth parameter that were held constant in all previous calculations.

Our result is plotted in Fig. 25. The differences in the two calculations for CALP are almost non-existent as shown in the follwoing table:

N1	=	3.0 mm (0.118 in)	3.6 mm (0.1416 in)
CALP-40	=	0.7313 (0.0088)	0.7269 (0.0089)
CALP-60	=	0.8682 (0.0068)	0.8620 (0.0069)

As a matter of curiosity, we made one factor at a time change to all other parameters that were held constant in PC-PRAISE, and found similar result, i.e., the difference was practically nil.

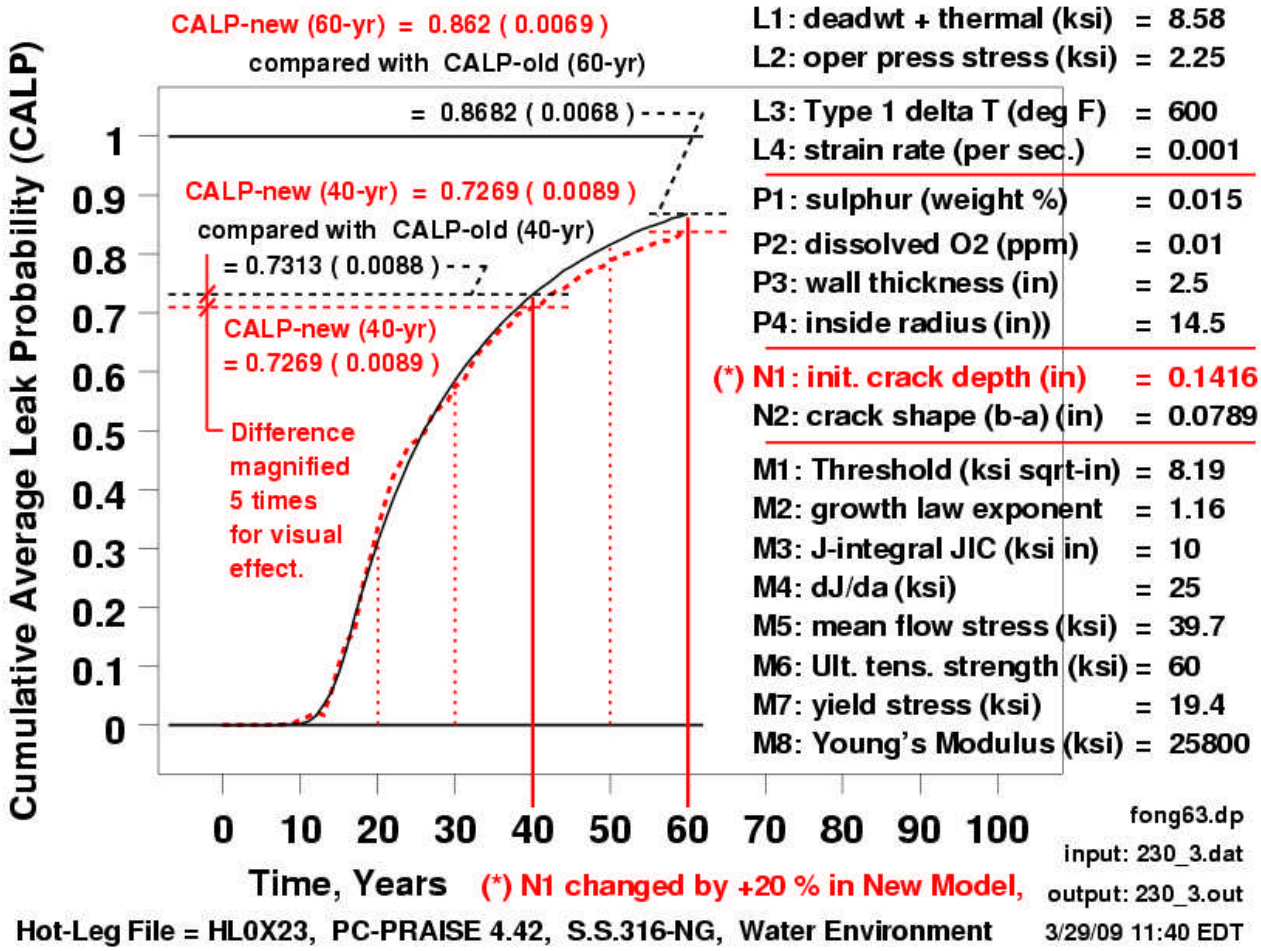

Fig. 25. A plot of the cumulative average leak probability (CALP) versus time based on the output file of a PC-PRAISE (v. 4.42) run using 4 distributional parameters, N2, M2, M5, and M6, and a non-distributional but 20%-increased parameter, N1, to compare with the same input without the 20% increase in N1.

VII. DESIGN OF EXPERIMENTS: DEX-1 (3 FACTORS)

The results of our last section using the so-called "one-factor-at-a-time" method prompted us to recall a statement made by Box, Hunter, and Hunter [43, p. 513], which reads as follows:

> " . . . the one-variable-at-a-time strategy fails . . . because it tacitly assumes that the maximizing value of one variable is independent of the level of the other. Usually this is not true."

In a complex model for crack growth involving close to 30 parameters, there are bound to be many possibilities of interaction and nonlinear effects when one attempts to find a relationship between source uncertainties and result uncertainty (see Eq. (1)). This is when we find the 2-level orthogonal factorial design of experiments approach attractive, because with only a few runs, not 10,000 in the case of PC-PRAISE, we will learn something about the f in Eq. (1).

So we set out to illustrate our approach with a design, to be called DEX-1, with three factors (k = 3) and full factorial (n = 2^3 = 8) with a center point making a total of 9 runs. Details of the complete design is shown in Table 3, where we vary by 10% each of the three factors, X1 (initial crack depth), X2 (crack growth law exponent), and X3 (crack growth law threshold K). The results of our 9 runs for five values of CALP are listed in Table 3 in red.

For each of the 5 columns of 9 red numbers in Table 3, we use our uncertainty plug-in, PD-UP, to run the DATAPLOT-10-Step-Analysis to obtain an estimated mean and 95% confidence bounds for each of the 20-, 30-, 40-, 50-, and 60-year times. Five of the10 plots generated by DATAPLOT for CALP-40 and the final result plot of uncertainty estimates are given in Figs. 26-31. In Fig. 32, we show a comparison of our DEX-1 run with similar PC-PRAISE run without the 10% perturbation, and the differences in leak-sigmas vary from a factor of 4 for CALP-60 to 6 for CALP-40.

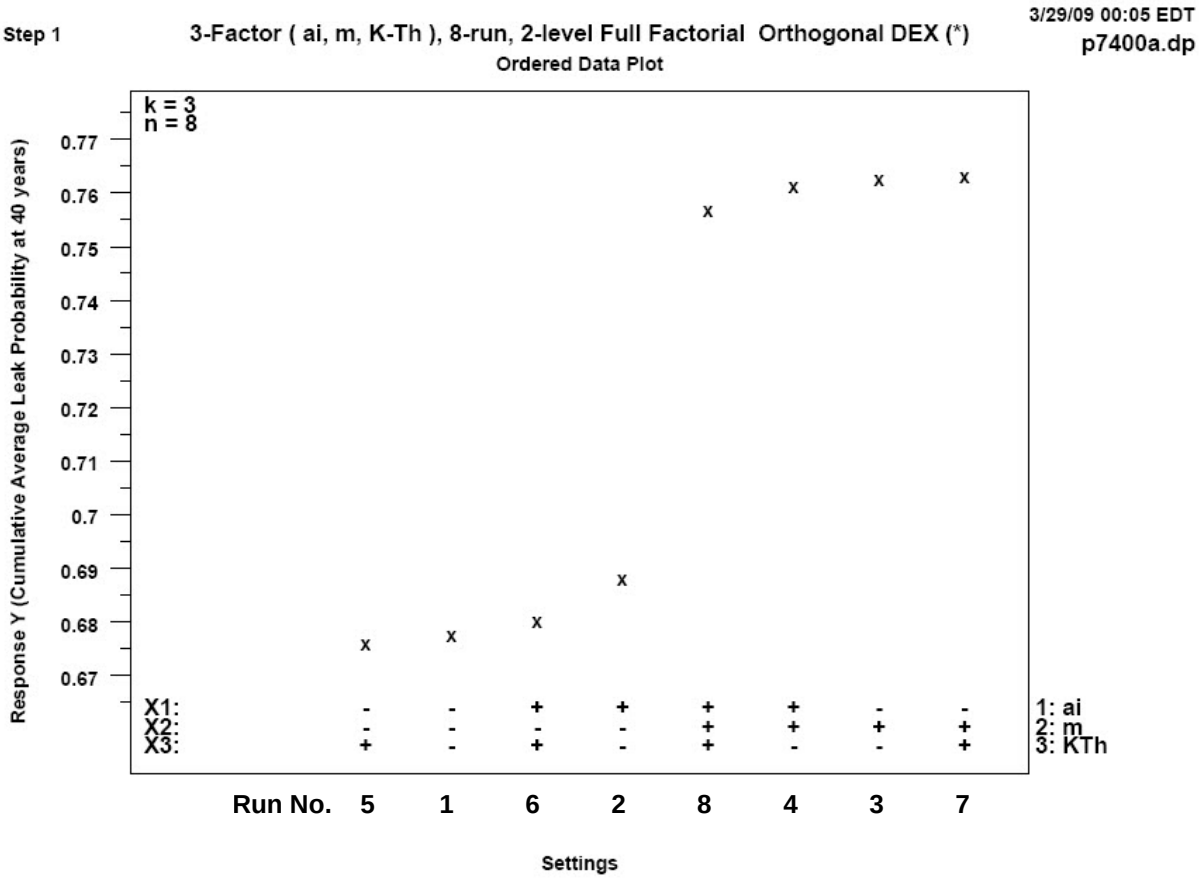

Fig. 26. First of 10 plots by the DATAPLOT-10-Step-Analysis [45] showing a plot of an ordered set of 8 values of CALP-40 without center point, as listed in Table 3 in red. Note the table at the bottom of the plot being the transposed DEX matrix with re-ordered columns as shown in Table 3.

Table 3. Details of a 3-Factor Full-Factorial Design (DEX-1) with 9 rows of PC-PRAISE results of CALP vs. Time (in red) and five columns of PD-UP Uncertainty Analysis results (in black)

	DEX-1 (k=3, n=8) X1 X2 X3 (ai, m, KTh)	20-year CALP	30-year CALP	40-year CALP	50-year CALP	60-year CALP	Ref. file-name
Center Point **Run-0** Factor Values	(0, 0, 0) (0.118, 1.16, 8.19)	0.3118	0.5856	0.7313	0.8155	0.8682	230_0
Assumed percent variation and a 2-level design of experiments	(10%, 10%, 10%) (-):(0.1062, 1.044, 7.371) (+):(0.1298, 1.276, 9.009)						
Run-1	(-1, -1, -1) (0.1062, 1.044, 7.371)	0.2114	0.5098	0.6782	0.7782	0.8385	100_X231
Run-2	(+1, -1, -1) (0.1298, 1.044, 7.371)	0.2215	0.5271	0.6887	0.7846	0.8469	100_X232
Run-3	(-1, +1, -1) (0.1062, 1.276, 7.371)	0.4025	0.6417	0.7631	0.8397	0.8806	100_X233
Run-4	(+1, +1, -1) (0.1298, 1.276, 7.371)	0.4093	0.6395	0.7617	0.8339	0.8788	100_X234
Run-5	(-1, -1, +1) (0.1062, 1.044, 9.009)	0.2042	0.5152	0.6764	0.7737	0.8370	100_X235
Run-6	(+1, -1, +1) (0.1298, 1.044, 9.009)	0.2221	0.5187	0.6807	0.7758	0.8381	100_X236
Run-7	(-1, +1, +1) (0.1062, 1.276, 9.009)	0.3961	0.6425	0.7635	0.8366	0.8798	100_X237
Run-8	(+1, +1, +1) (0.1298, 1.276, 9.009)	0.4072	0.6419	0.7574	0.8289	0.8791	100_X238
DEX-1 (k=3,n=8) Estimated Mean		0.3096	0.5802	0.7223	0.8074	0.8608	
DEX-1 (k=3,n=8) 95% Lower Bound		0.1867	0.4998	0.6699	0.7703	0.8349	
DEX-1 (k=3,n=8) 95% Upper Bound		0.4324	0.6607	0.7748	0.8446	0.8867	

PC-PRAISE Result for Run-1

PD-UP Uncertainty Analysis Result for CALP-40

VII. DEX-1: K = 3, N = 8 (CONT'D)

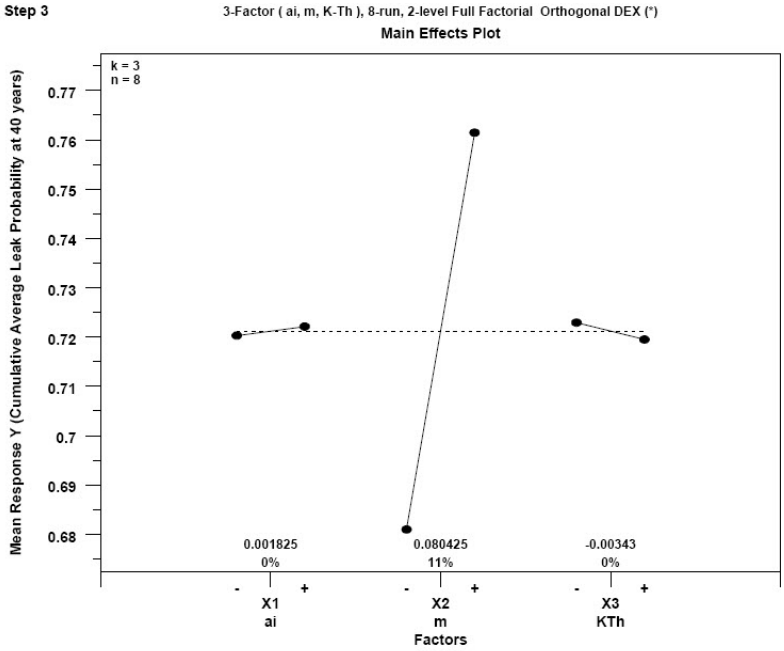

Fig. 27. Third of 10 plots by the DATAPLOT-10-Step-Analysis [45] showing the main effects on CALP-40 due to a 10% change in each of the three factors, X1, X2, and X3. Note the dominance of factor X2, the crack growth exponent m .

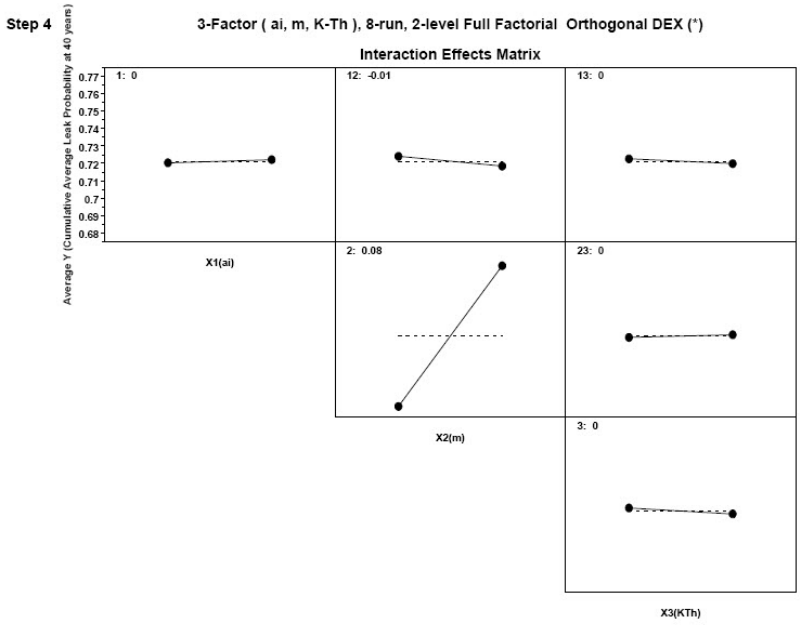

Fig. 28. Fourth of 10 plots by the DATAPLOT-10-Step-Analysis [45] showing the interaction matrix of a first order 3-parameter model. The boxes on the main diagonal are re-plots of the results of Fig. 27. Interactions are small.

VII. DEX-1: K = 3, N = 8 (CONT'D)

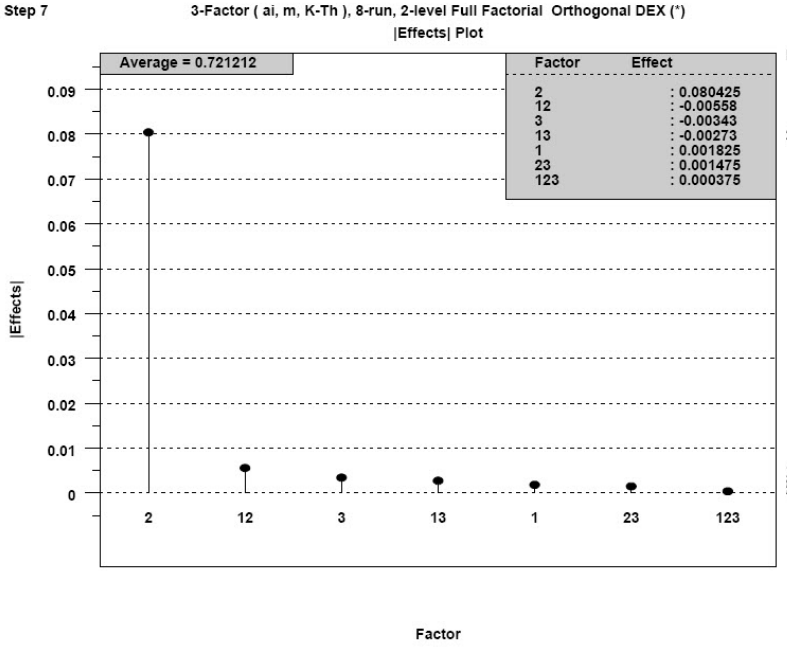

Fig. 29. Seventh of 10 plots by the DATAPLOT-10-Step-Analysis [45] showing a ranking of the absolute values of all one-way and two-way effects of the 8-run dataset for a full factorial orthogonal DEX with k=3 and n=8.

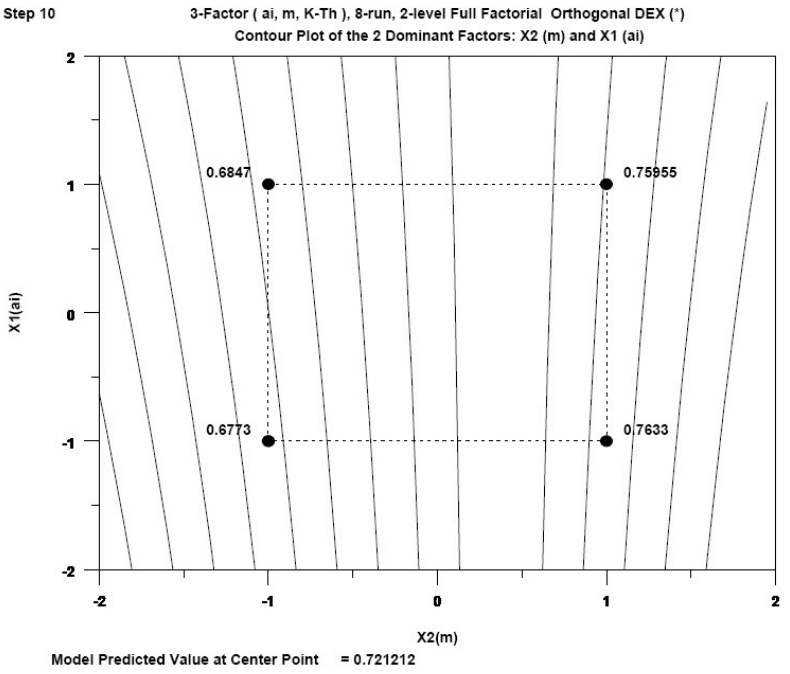

Fig. 30. Step 10 of the DATAPLOT-10-Step-Analysis shows a contour plot of a linear least-square model of two dominant parameters, X1 and X2. The relative plane behavior of the plot confirms that the interactions are small.

VII. DEX-1: K = 3, N = 8 (CONT'D)

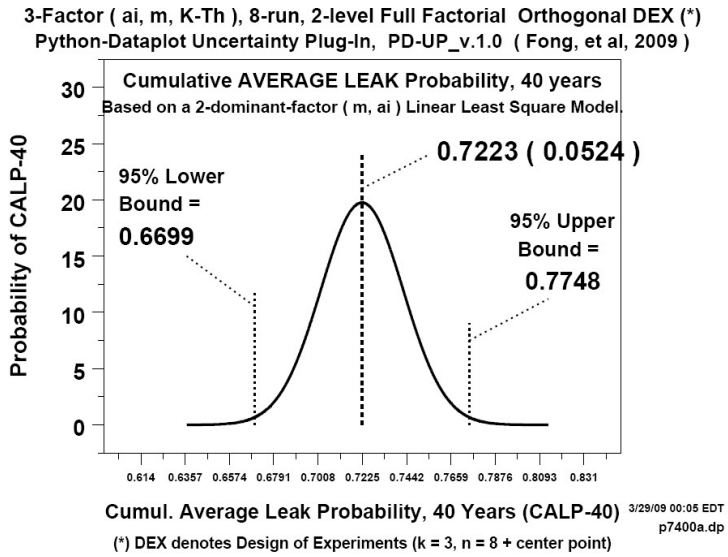

Fig. 31. A probabiliy plot of CALP-40 based on a linear regression fit of the 9-run results (see Table 3 in red) with two dominant factors, X1 and X2, selected from the ranking plot of Fig. 27. The results are also tallied in Table 3.

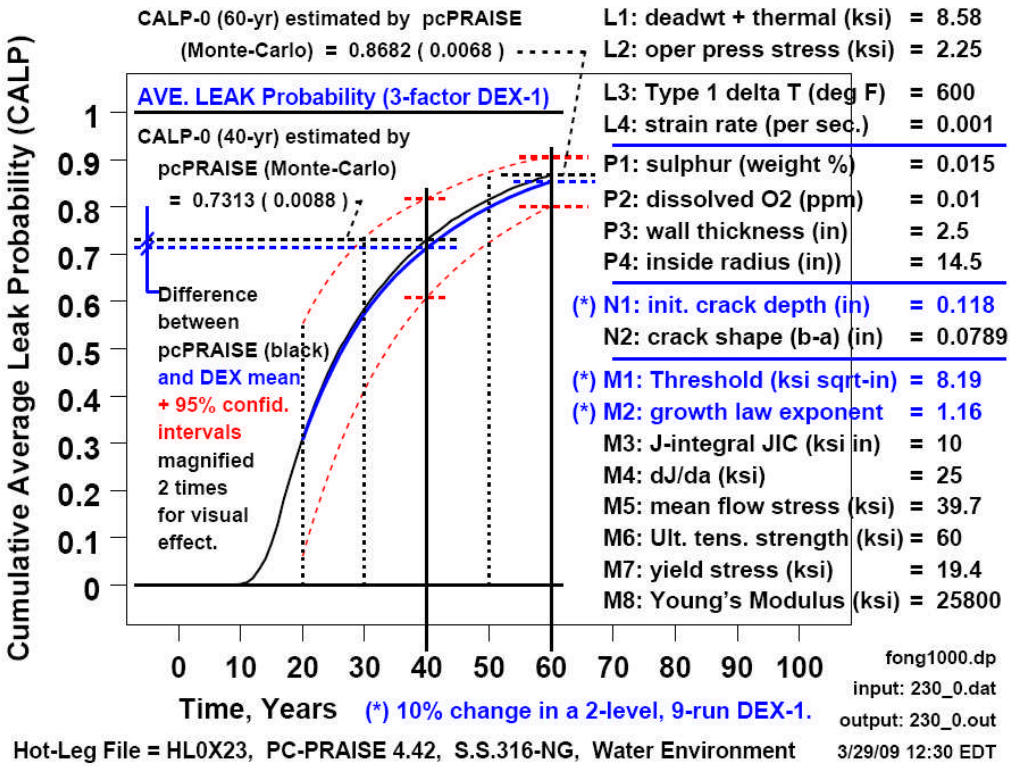

Fig. 32. A plot of CALP vs. time based on a 3-factor, full factorial, 8-run+center-point design (DEX-1) with a 10% variation in each of three factors, N1, M1, and M2, as compared with the same plot given in Fig. 24. The estimated mean and confidence half-interval of the DEX-1 run differ sharply from similar PC-PRAISE run of [17].

VIII. DESIGN OF EXPERIMENTS: DEX-2 (3 FACTORS)

In the last section, we conducted a 3-factor, full-factorial design of experiments (**DEX-1**) by varying just **10%** of each of the three selected factors, and obtained dramatic changes in the 95% confidence half-intervals of CALP at all time values, as compared with the baseline results, i.e., the same PC-PRAISE run without the 10% change. A summary of the comparison is given in the following table :

CALP-Year	Baseline Mean (2*leak-σ)	**DEX-1 Mean** (c-half-int)	**Ratio =** (c-half-int) / 2*leak-σ
CALP-20	0.3118 (0.0092) **	**0.3096** (0.1229)	13.4
CALP-30	0.5856 (0.0098)**	**0.5802** (0.0804)	8.2
CALP-40	0.7313 (0.0088) **	**0.7223** (0.0524)	6.0
CALP-50	0.8155 (0.0078) **	**0.8074** (0.0371)	4.8
CALP-60	0.8682 (0.0068) **	**0.8608** (0.0259)	3.8

** 95% confidence half-interval for baseline is 2*leak-σ , where leak-σ is listed in Table 2.

For a discussion on the size of the changes we impose on the three factors, let us recall from Table 3 the following information on the three factors chosen for **DEX-1** with their base values and 2-level changes:

Process Factor (Name of Parameter)	Base Value	Incre-ment	**DEX-1** (-)	**DEX-1** (+)
X1 (initial crack depth)	0.118	**10%**	0.1062	0.1298
X2 (growth exponent)	1.16	**10%**	1.044	1.276
X3 (ΔK threshold)	8.19	**10%**	7.371	9.009

A 10% change in X1 (initial crack depth) varies its value from 3.0 mm (0.118 in) at its center point to a low of 2.7 mm and a high of 3.3 mm. From our past NDE studies [24, 32, 33], we believe the change is too small and not realistic. An alternative amount, say, **40%**. that would result in a low of 1.8 mm and a high of 4.2 mm, seems more reasonable and will be adopted for our next investigation, i.e., **DEX-2**.

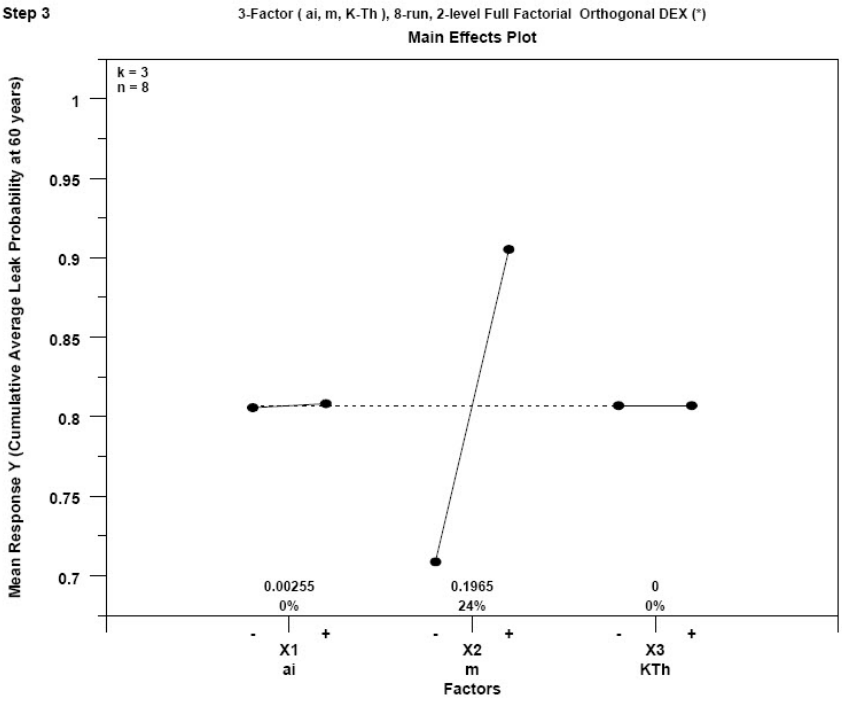

Fig. 33. Third of 10 plots by the DATAPLOT-10-Step-Analysis [45] showing the main effects on CALP-40 due to a 40% change in X1 (initial crack depth), 40% change in X2 (exponent m), and 20% change in X3 (K threshold). Note the increased dominance of factor X2 (the crack growth exponent m) in DEX-2 as compared with DEX-1.

VIII. DEX-2: K = 3, N = 8 (CONT'D)

Along the same line of argument, a 10% change in X2 (crack growth law exponent *m*) varies its value from 1.16 at its center point to a low of 1.044 and a high of 1.276. From our past studies [33] and the literature (see, e.g., [70] and Fig. 13 in Section IV), we believe the change is also too small and not realistic. An alternative amount, say, **40%**. that would result in a low of 0.70 and a high of 1.62, seems more reasonable and will be adopted for our next case study, i.e., **DEX-2**. Similarly,

a 10% change in X3 (ΔK threshold) varies its value from 8.19 at its center point to a low of 7.37 and a high of 9.10. From our past studies [68, 69] and the literature (see, e.g. [71, 72] and Figs. 15 and 16 in Sect. IV), that is also too small. An alternative amount, say, **20%**. that would result in a low of 6.55 and a high of 9.83, will be adopted for **DEX-2**.

As shown in Figs. 33 & 34, the results of our DEX-based investigation is quite dramatic. The DEX-2 results not only drastically changed the ratio of the its confidence half-interval to that of the baseline at each time year, but also the ratio of the two estimated means. A list of those two ratios is given below:

CALP-Year for **DEX-2**	Ratio of the Means	Ratio of the Confidence Half-Interval
CALP-20	(##)	(##)
CALP-30	0.83	32.9
CALP-40	0.88	26.3
CALP-50	0.91	22.0
CALP-60	0.94	19.0

(##) DEX-2 run failed to estimate the mean and uncertainty bounds of CALP-20 because the regression fit using two dominant factors did not produce a reasonable plane contour plot.

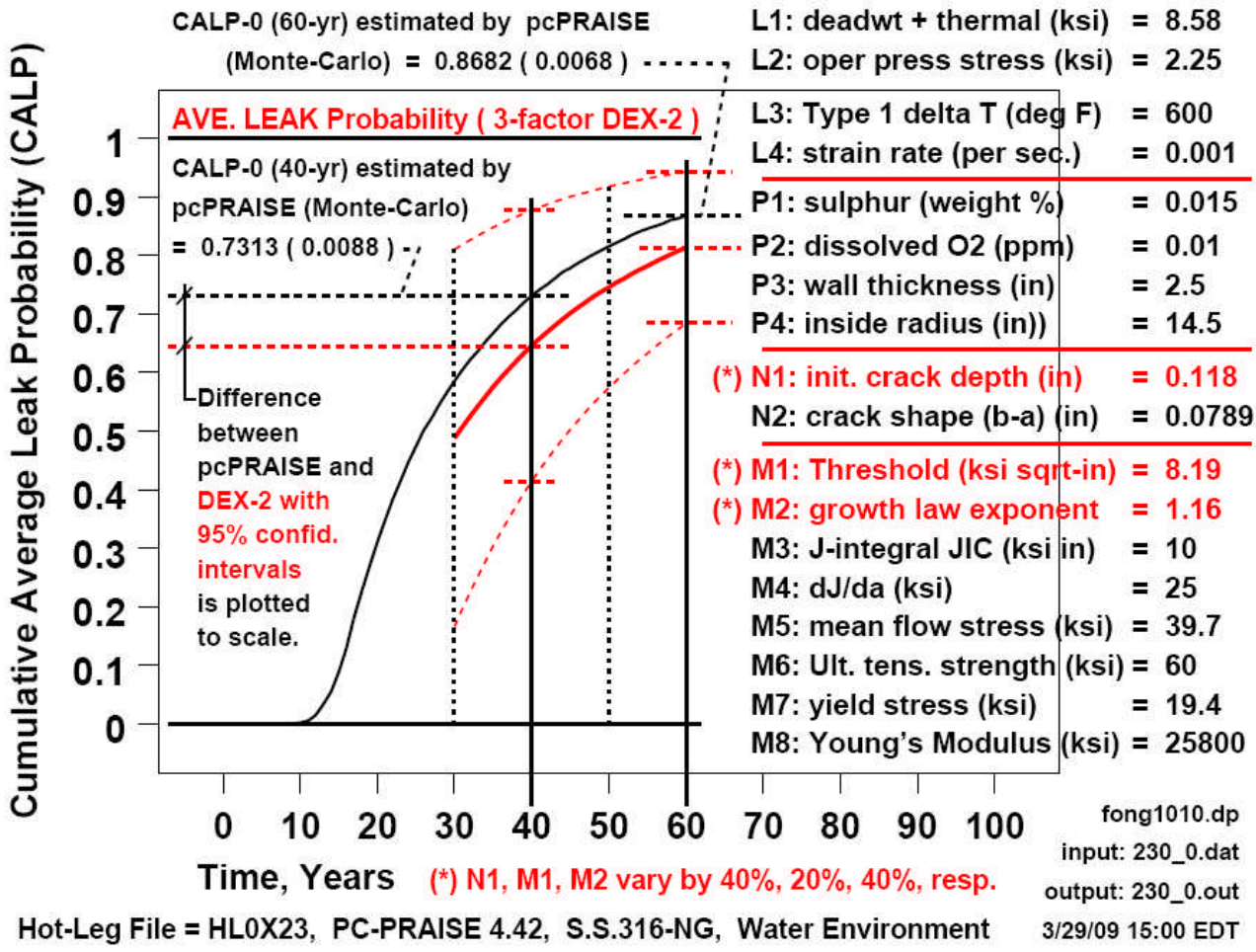

Fig. 34. A plot of CALP vs. time based on a 3-factor, full factorial, 8-run+center-point design (DEX-2) with a 40% change in N1, 40% change in M1, and 20% change in M2, as compared with the same plot given in Fig. 24. The estimated mean and confidence half-interval of the DEX-2 run differ sharply from similar PC-PRAISE run of [17].

IX. DESIGN OF EXPERIMENTS: DEX-3 (5 FACTORS)

In the last two sections, we introduced two full factorial designs, because for a three-factor experiment (k = 3), a full factorial design requires $n = 2^3$ (= 8), a reasonably small number for conducting a virtual experiment.

In the next two sections, we will describe an exercise of pushing our DEX approach to its limit by keeping n to a maximum of 8 and ask for two different values of k, i.e., 5 and 7. Note that the number of factors, k, is required to be always less than the number of runs, n, so $k = 7$ is the most we can do for $n = 8$.

In this section, we will work with $k = 5$ and $n = 8$ (**DEX-3**). In addition to the three factors we already selected in DEX-1 and DEX-2, we need to add two more factors, X4 and X5, to make $k = 5$. A full factorial DEX for $k = 5$ requires 2^5 (=32) runs. A 5-factor, 8-run DEX is known as a fractional factorial orthogonal design, which is more economical but not as accurate, because a DATAPLOT-10-Step-Analysis will show in its 7th plot complications due to the confounding of one-way and two-way effects of a first-order model (see Fig. 29 for an example of this difficulty and also Ref. [43, p.338]).

As Box, Hunter, and Hunter said in Ref. [43, p.338], ". . . we have to give up something to get something." A fractional factorial design works to one's favor if the two-way effects are small, and the results of the analysis will be close to those of the full factorial design (a 32-run vs. the cheaper 8-run experiment).

Since our crack growth model deals with the formation of a through wall crack (crack depth greater than wall thickness), we thought we might choose to vary the parameter, P3, in the list of parameters exhibited in Fig. 34. We also came to the conclusion that if P3 (wall thickness), being a measurable geometric parameter, is allowed to vary by, say, **5%**, we should also expect another geometric parameter, P4 (inner radius), to vary by the same amount. Our final design for **DEX-3** (k = 5, n = 8) will assume the following form:

	X1	X2	X3	X4	X5
Base value =	0.118	1.16	8.19	2.50	14.5
% change =	40	40	20	5	5
low value (-) =	0.0708	0.696	6.552	2.375	13.775
high value (+) =	0.1652	1.624	9.828	2.625	15.225

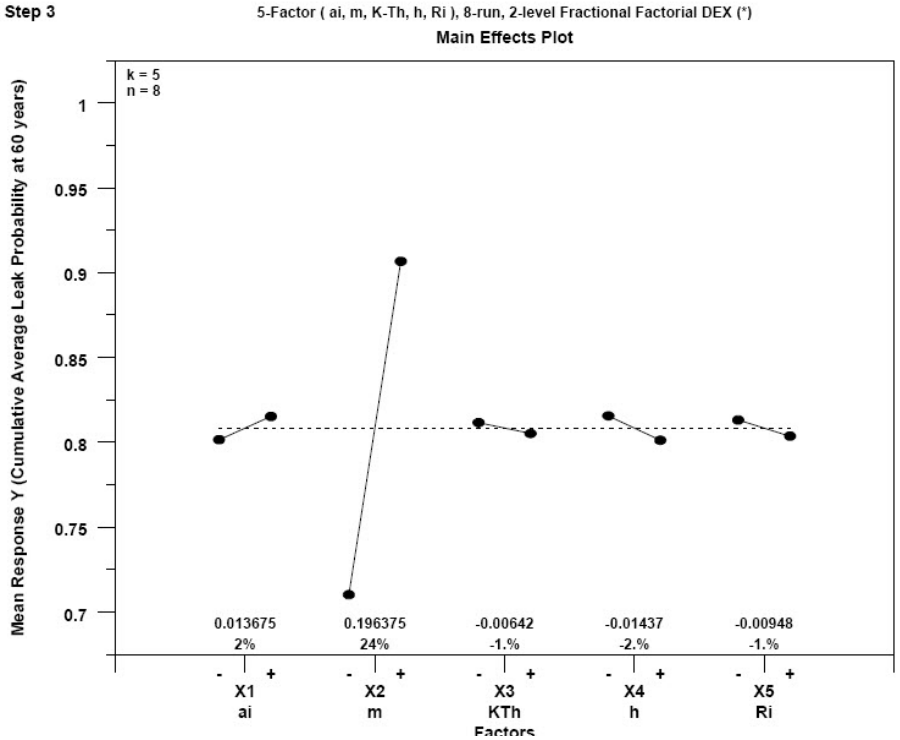

Fig. 35. Third of 10 plots by the DATAPLOT-10-Step-Analysis [45] showing the main effects on CALP-40 due to a 40% change in X1 (initial crack depth), 40% change in X2 (exponent m), 20% change in X3 (K threshold), 5% change in X4 (wall thickness), and 5% change in X5 (inner radius). Note the continued dominance of factor X2 (the crack growth exponent m) in DEX-3 as compared with DEX-2.

IX. DEX-3: K = 5, N = 8 (CONT'D)

We are now ready to use our uncertainty plug-in, PD-UP, to take over the task of assigning the various combinations of low's and high's, i.e., the (-)'s and the (+)'s , to each run according to the following table (see Fig. 23 for same):

Order of Run	X1	X2	X3	X4	X5
1	- 1	- 1	- 1	+ 1	+ 1
2	+1	- 1	- 1	- 1	- 1
3	- 1	+1	- 1	- 1	+ 1
4	+1	+1	- 1	+ 1	- 1
5	- 1	- 1	+1	+ 1	- 1
6	+1	- 1	+1	- 1	+ 1
7	- 1	+1	+1	- 1	- 1
8	+1	+1	+1	+ 1	+ 1

The reader may wish to verify that the first three columns for an 8-run table are the same as those of a full factorial one (see Subsection 5.4), the fourth column is the product of the first two columns, and the fifth column is the product of the first and third columns. Such algorithm is to ensure that the design is orthogonal. With the appropriate values of the five factors for each run in place, we conduct 8 new runs of PC-PRAISE and obtain 8 time histories of the values of CALP similar to a list of red numbers given in Table 3 for **DEX-1**. We are now ready to run DATAPLOT-10-Step-Analysis using PD-UP to obtain CALP mean and 95% confidence intervals as shown below:

CALP-Year for **DEX-3**	Ratio of the Means	Ratio of the Confidence Half-Interval
CALP-30	0.83	33.1
CALP-40	0.88	26.4
CALP-50	0.92	22.1
CALP-60	0.94	19.1

The plots of Figs. 35 & 36 show the significance of the 2 ratios.

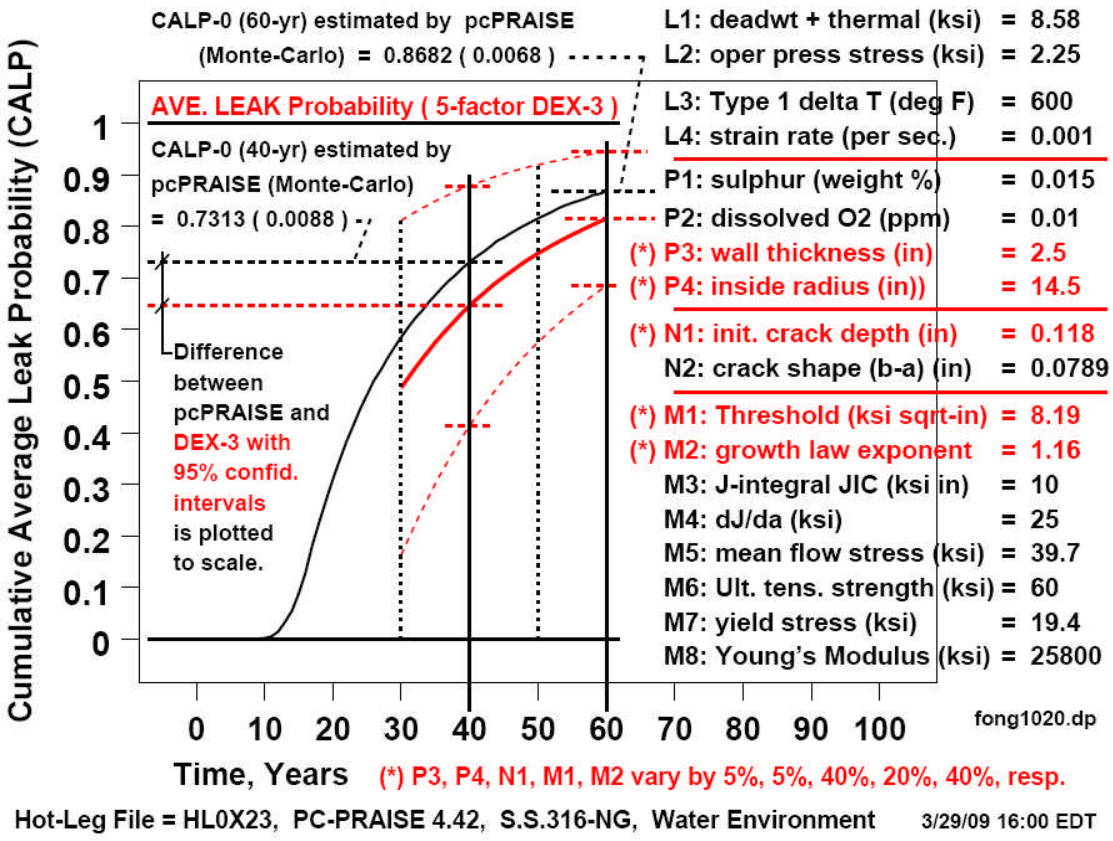

Fig. 36. A plot of CALP vs. time based on a 5-factor, fractional factorial, 8-run+center-point design (DEX-3) with a 40% change in N1, 40% change in M1, 20% change in M2, 5% change in P3, and 5% change in P4, as compared with the same plot given in Fig. 24. The estimated mean and confidence half-interval of the DEX-3 run differ sharply from similar PC-PRAISE run of [17].

X. DESIGN OF EXPERIMENTS: DEX-4 (7 FACTORS)

In Fig. 36, we note on its right a list of 18 factors with their labels identified as four ***L***'s, four ***P***'s, 2 ***N***'s and 8 ***M***'s according to a notation given in Table 1.

For **DEX-1** and **DEX-2** (k = 3), we chose one factor, **N1**, from the NDE database. ***DB-2***, and two factors, **M1** and **M2**, from the material property database, ***DB-3***.

For **DEX-3** (k = 5), we chose two factors, **P3** and **P4**, from the physical-chemical-composition database, again one factor, **N1**, from the NDE database. ***DB-2***, and two factors, **M1** and **M2**, from the material property database, ***DB-3***.

For the final case, **DEX-4** (k = 7), we will add two more factors from the list of 18 (Fig. 36). Since crack growth is definitely a function of loads and loading rates, both mechanical and thermal, we choose **L1** (deadweight plus thermal stress) and **L4** (strain rate) from the loading and constraint database.

We also believe that a **10%** variation in both **L1** and **L4** is reasonable. The final design for **DX-4** (k = 7, n = 8) assumes the following form:

	X1	X2	X3	X4	X5	X6	X7
Base value	0.118	1.16	8.19	2.50	14.5	8.58	0.001
% change 10		40	40	20	5	5	10
low (-)	0.0708	0.696	6.552	2.375	13.775	7.722	0.0009
high (+)	0.1652	1.624	9.828	2.625	15.225	9.438	0.0011

Once again, we let our uncertainty plug-in, PD-UP, do the work of assigning the various combinations of low's and high's to each of the 8 runs according to the following table:

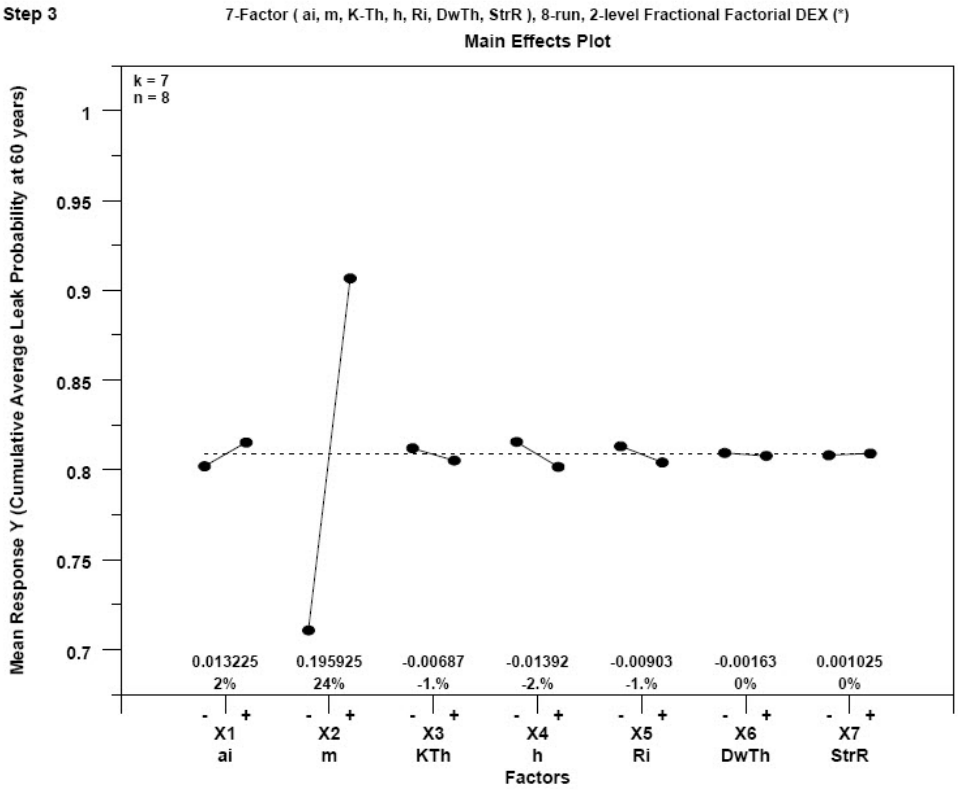

Fig. 37. Third of 10 plots by the DATAPLOT-10-Step-Analysis [45] showing the main effects on CALP-40 due to a 40% change in X1 (initial crack depth), 40% change in X2 (exponent m), 20% change in X3 (K threshold), 5% change in X4 (wall thickness), 5% change in X5 (inner radius), 10% change in X6 (deadweight plus thermal), and 10% change in X7 (strain rate). Note the continued dominance of factor X2 (the crack growth exponent m) in DEX-4 (7-factor, 8-run) as compared with DEX-3 (5-factor, 8 run).

X. DEX-4: K = 7, N = 8 (CONT'D)

Order of run	X1	X2	X3	X4	X5	X6	X7
1	-1	-1	-1	+1	+1	+1	-1
2	+1	-1	-1	-1	-1	+1	+1
3	-1	+1	-1	-1	+1	-1	+1
4	+1	+1	-1	+1	-1	-1	-1
5	-1	-1	+1	+1	-1	-1	+1
6	+1	-1	+1	-1	+1	-1	-1
7	-1	+1	+1	-1	-1	+1	-1
8	+1	+1	+1	+1	+1	+1	+1

Again the reader may wish to verify that the first five columns of the above are the same as those of **DEX-3** ($k = 5$, $n = 8$), the 6th column is the product of the 2nd and 3rd columns, and the 7th column is the product of the first three columns. With the appropriate values of the seven factors for each run in place, we conduct 8 new runs of PC-PRAISE and obtain 8 time histories of the values of CALP similar to a list of red numbers given in Table 3 for **DEX-1**. We are now ready to run DATAPLOT-10-Step-Analysis using PD-UP to obtain CALP mean and 95% confidence intervals as shown below:

CALP-Year for **DEX-4**	Ratio of the Means	Ratio of the Confidence Half-Interval
CALP-30	0.83	33.1
CALP-40	0.88	26.4
CALP-50	0.92	22.0
CALP-60	0.94	19.0

The plots of Figs. 37 & 38 show the significance of the 2 ratios.

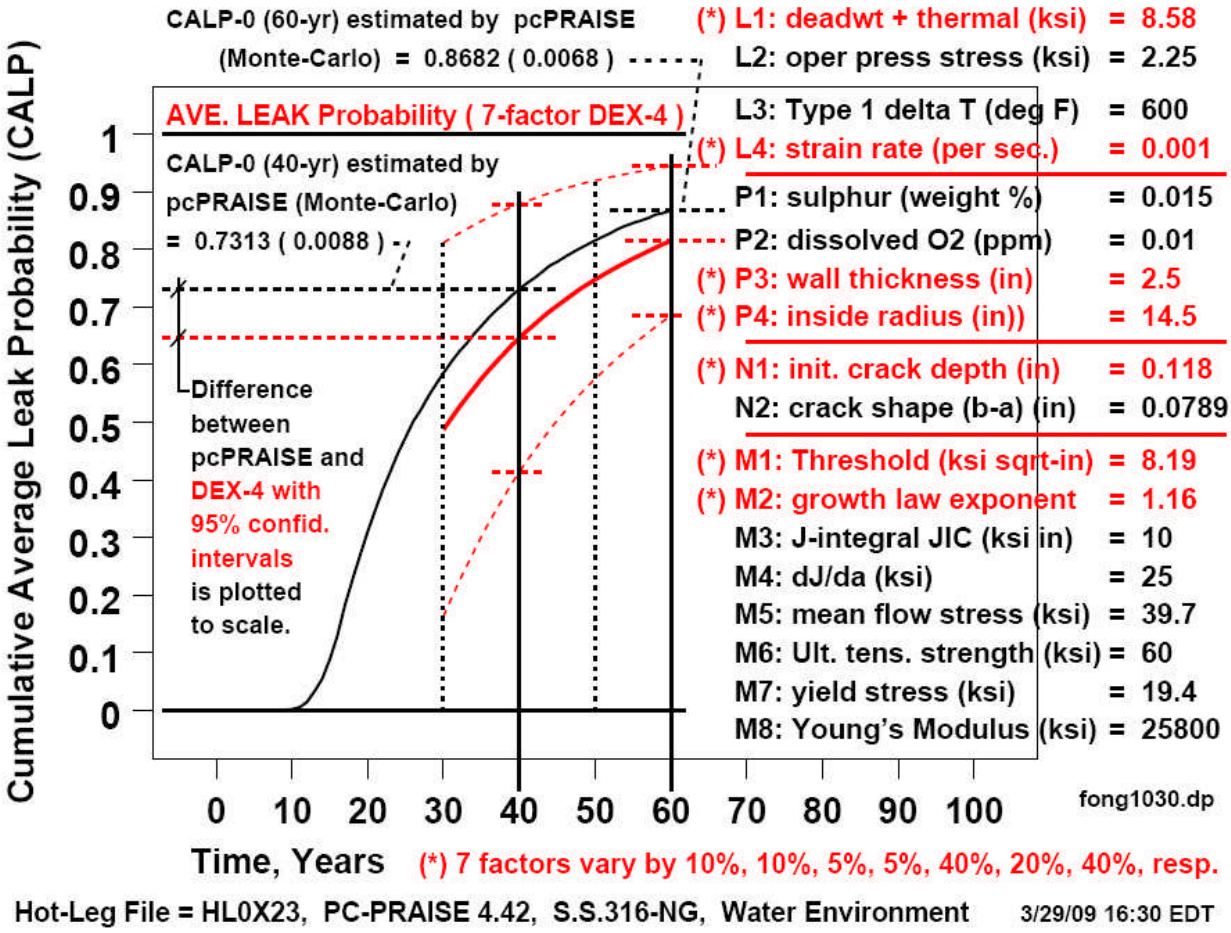

Fig. 38. A plot of CALP vs. time based on a 7-factor, fractional factorial, 8-run+center-point design (DEX-4) with a 40% change in N1, 40% change in M1, 20% change in M2, 5% change in P3, 5% change in P4, 10% change in L1, and 10% change in L4, as compared with the same plot given in Fig. 24. The estimated mean and confidence half-interval of the DEX-4 run differ sharply from similar PC-PRAISE run

XI. SIGNIFICANCE OF RESULTS

In this paper, we have developed an economical and efficient methodology in relating six categories of source uncertainties in a class of mathematical models to the result uncertainty of a specific model under investigation.

We have also demonstrated the usefulness of this methodology by applying it to a probabilistic Monte-Carlo-based model of fatigue crack growth using a public-domain PC-version [17] of a Fortran software package named PRAISE (an acronym for Piping Reliability Analysis Including Seismic Events).

Using an uncertainty estimation plug-in [49] to illustrate our application with four examples, we have also shown that our methodology, which is based on the statistical theory of design of experiments [43], is not only economical in terms of a minimum requirement for a simulation experiment to obtain the model result uncertainty, but also more versatile than the Monte-Carlo method, because our method provides the user a capability to

(a) study model parametric interactions including two-term effects,

(b) rank the relative importance of various parameters and their interactions suspected of significantly contributing to the model result uncertainty, and

(c) devise a sequential screening strategy to benchmark and improve model performance.

As an example of capability (c), we have demonstrated that, in all four case studies involving a fatigue crack growth model, the leak probabiliity, CALP, of a stainless steel pipe in a nuclear power plant has a significantly larger uncertainty using our method than the Monte-Carlo method of PC-PRAISE. Depending on the magnitude of the two-level variation of factors in a full or fractional factorial experimental design, the ratio of the confidence half-interval of our prediction to that of the PC-PRAISE varies from a low of 4 for CALP (Year 60) to a high of 33 for CALP (Year 30). Such discrepancy is not intended to discredit the Monte-Carlo results of PC-PRAISE, but to shed more light on the performance and efficacy of a complex model.

Consequently, the methodology presented in this paper is significant to engineers who will be able to better manage aging structures with uncertainty-analysis-included models capable of (a) ranking the relative importance of source uncertainties, (b) estimating the result uncertainty, and (c) continuously benchmarking such models with up-to-date information from failure event databases (***DB-1***).

XII. CONCLUDING REMARKS

This paper concludes a 4-part series on solving a basic question in computer-aided maintenance engineering. Using the methodology outlined in this series of papers and supported by information from five different but inter-related databases as defined in Table 1, the owner and operator of an aging structure will be able to estimate the remaining useful life of a structure or equipment at a level of confidence appropriate to its designed purpose.

To reiterate, we have shown in Part 1 [50], that an artificial intelligence (AI) tool named ANLAP [53] and a statistical analysis package named DATAPLOT [45] can be applied to automatically extract data from unstructured text in failure event reports and enhance the value of a failure mechanism database by minimizing human errors in data entry and segmentation. This addresses ***DB-1***.

In Part 2 [51], where we address ***DB-2***, a web-based uncertainty plug-in (WUPI) can link inservice inspection (ISI) reports with service flaw location and sizing databases such that properly entered and segmented NDE data can be statistically analyzed and formatted for dissemination as input to fatigue life prediction modeling.

In Part 3 [52], where we address ***DB-3***, a Dataplot-Python-Anlap plug-in can link testing reports with databases such that properly entered and segmented material property data can be statistically analyzed and formatted for dissemination as input to fatigue life prediction modeling.

Using the information on source uncertainties from five different types of databases, i.e., ***DB-1***, ***DB-2***, ***DB-3***, a loads/constraints database, and a physical-chemical-composition database, we show in this paper a methodology to estimate the result uncertainty of a remaining life prediction model as an example to solve the aging structure maintenance problem.

XIII. REFERENCES

1. U.S. Nuclear Regulatory Commission, 2008, Fact Sheet on the Three Mile Island Accident. USNRC, Washington, DC, http://www.nrc.gov/reading-rm/doc-collections/fact-sheets/3mile-isle.html (2008).
2. Fong, J. T., 1980, "Inservice Data Reporting Standards for Engineering Reliability and Risk Analysis," Nucl. Eng. Design, Vol. 60, No. 1, pp. 159-161 (1980).
3. Fong, J. T., 1986, "Integration of Engineering Analysis and Databases for Critical Decision Making," Computers in Mechanical Engrg. (CIME), Vol. 5 (1), 42-55 (1986).
4. Fong, J. T., and Bernstein, B., 1988, "Building a PC-Based Knowledge Base for Improving NDE Reliability," in Pressure Vessel Technology, Proc. 6th Int'l Conf. On

Pressure Vessel Technology, Beijing, China, Sep. 11-15, 1988, C. Liu and R. W. Nichols, eds., Vol. II, pp. 1349-1371. Pergamon (1988).

5. Vo, T. V., Gore, B. F., Eschbach, E. J., and Simonen, F. A., 1989, "Probabilistic Risk Assessment Based Guidance for Piping Inservice Inspection," Nuclear Technology, Vol. 88, pp. 13-20 (1989).
6. Doctor, S. R., and Spanner, J. C., Sr., 1993, "Studies on the Quantification of NDE Reliability," Proc. ASME 1993 PVP Conference, Spec. Pub. PVP-Vol. 257 entitled "Scientific and Engineering Aspects of Nondestructive Evaluation," pp. 39-46 (1993).
7. Bush, S.H., Do, M.J., Slavich, A.L., Chockie, A.D., 1996, Piping Failures in United States Nuclear Power Plants: 1961-1995, SKI 96:20, prepared by the Chockie Group Int'l, Inc., Seattle, WA, for the Swedish Nuclear Power Inspectorate, Stockholm, Sweden, (1996)
8. EPRI TR-106706, 1996, Risk-Informed Inservice Inspection Evaluation Procedure, Electric Power Research Institute, Inc. Palo Alto, California. (1996)
9. ASME Code Case N-577, 1997, Risk-Informed Requirements for Class 1, 2, and 3 Piping, Method A. New York, NY: ASME (1997).
10. Bush, S. H., 1997, "Interpretive Report on Nondestructive Examination Techniques, Procedure for Piping and Heavy Section Vessels," Welding Research Council Bulletin 420, April 1997, Welding Research Council, NY, NY (1997).
11. Zhao, Z., and Haldar, A., 1997, "Reliability-based Structural Fatigue Damage Evaluation and Maintenance Using Non-destructive Inspections," in Uncertainty Modeling in Finite Element, Fatigue and Stability of Systems, A. Haldar, A. Guran, and B. M. Ayyub, Eds., pp. 159-214. World Scientific Publishing Company, River Edge, NJ 07661 (1997).
12. EPRI, 1998, Nuclear Reactor Piping Failures at U.S. Commercial LWRs: 1961-1997, TR-110102, Electric Power Research Institute, Palo Alto, CA (1998)
13. Schuster, G. J., Doctor, S. R., Heasler, P. G., 1998, Characterization of Flaws in U.S. Reactor Pressure Vessels: Density and Distribution of Flaw Indications in PVRUF, NUREG/CR-6471, Vol. 1. U.S. Nuclear Regulatory Commission, Washington, DC (1998).
14. U.S. Department of Energy, 1998, Operating Experience Weekly Summary 98-40, October 2 through October 8, 1998, published by the U. S. Department of Energy, Office of Environment, Safety and Health, and its Office of Nuclear and Facility Safety (NFS) and Office of Operating Experience Analysis and Feedback (OEAF), http://tis.eh.doe.gov/web/oeaf/oe_weekly.html (1998).
15. Khaleel, M. A., and Simonen, F. A., 1999, "Uncertainty Analyses for Calculated Failure Probabilities of Piping Welds," in Proc. ASME PVP Conference, Boston, MA, Aug. 1-5, 1999, PVP Vol. 383, entitled "Pressure Vessel and Piping Codes and Standards, 1999," B. T. Lubin, et al, eds., pp. 77-90. American Society of Mechanical Engineers, New York, NY 10016 (1999).
16. Westinghouse, 1999, Westinghouse Owners Group Application of Risk-Informed Methods to Piping Inservice Inspection Topical Report, WCAP-14572, Revision 1, NP-A Westinghouse Energy Systems, Pittsburgh, PA, (1999)
17. Khaleel, M. A., Simonen, F. A., Phan, H. K., Harris, D. O., and Dedhia, D., 2000, Fatigue Analysis of Components for 60-year Plant Life, NUREG/CR-6674. U. S. Nuclear Regulatory Commission, Washington DC (2000).
18. U.S. Nuclear Regulatory Commission, NUREG-1801, 2001, Vo. 1 Rev. 0, Generic Aging Lessons Learned (GALL) Report, Nuclear Regulatory Commission, Washington DC (2001).
19. API, 2002, API 580 Risk-Based Inspection. Washington, D.C.: American Petroleum Institute (2002).
20. Simonen, F. A., Schuster, G. J., Doctor, S. R., and Dickson, T. L., 2002, "Distributions of Fabrication Flaws in Reactor Pressure Vessels for Structural Integrity Evaluations," Proc. ASME PVP Conf., Vancouver, BC, Canada, Aug. 5-9, 2002, Spec. Pub. PVP-Vol. 443-2, Fatigue, Fracture, and Damage Analysis, Vol. II, pp. 125-131. ASME (2002).
21. Gosselin, S. R., et al, 2005, "Performance Demonstration Based Probability of Detection (POD) Curves for Fatigue Cracks in Piping," paper PVP2005-71027, Proceedings of, ASME PVP 2005 Conf., Denver, CO. ASME (2005).
22. Lydell, B.O.Y., 2005, PIPExp/PIPE-2005: Monthly Summary of Database Content (Status as of Dec-2005), RSA-R-2005-01.07, Sigma-Phase Inc. Tucson AZ, (2005)
23. Nyman, R. et al., 2005, "Reliability of Piping System Components Framework for Estimating Failure Parameters from Service Data", SKI Report 97:26 3rd edition, Swedish Nuclear Power Inspectorate, Stockholm, Sweden, (2005)
24. Fong, J. T., and Hedden, O. F., eds., 2007, Engineering Safety, Applied Mechanics, and Nondestructive Evaluation (NDE), Proc. 2007 ASME PVP Symp in honor of Dr. Spencer H. Bush (1920-2005), July 25-26, 2007, San Antonio, TX. Published by Stanford Mechanics Alumni Club, 104 King Farm Blvd, Suite C308, Rockville, MD 20850 (2007).
25. Lydell, B.O.Y., 2007a, "The Probability of Pipe Failure on the Basis of Operating Experience," PVP2007-26281, Proc. 2007 ASME Pressure Vessel and Piping Division Conference, July 22-26, 2007, San Antonio, TX (2007a).
26. Simonen, F. A., Doctor, S. R., Gosselin, S. R., Rudland, D. L., Xu, H., Wilkowski, G. M., and Lydell, B. O. Y., 2007a,

Probabilistic Fracture Mechanics Evaluation of Selected Passive Components - Technical Letter Report, a Pacific Northwest National Laboratory Report PNNL-16625 dated May 2007, prepared for the U.S. Nuclear Regulatory Commission, Washington, DC 20555 (2007a).

27. Simonen, F. A., Gosselin, S. R., Lydell, B. O. Y., Rudland, D. L., and Wilkowski, G. M., 2007b, "Application of Failure Event Data to Benchmark Probabilistic Fracture Mechanics Computer Codes," Proceedings of ASME 2007 PVP Conference, San Antonio, TX, July 22-26, Paper No. PVP2007-26373. ASME, New York, NY (2007b).

28. U.S. Nuclear Regulatory Commission, NUREG/CR-6945, 2007, Fabrication Flaw Density and Distribution in Repairs to Reactor Pressure Vessel and Piping Welds, Nuclear Regulatory Commission, Washington DC (2007).

29. Chockie, A. D., and Gregor, F. E., 2008, "The Role of Failure Data in Plant Aging Management and Life Extension," Proc. ASME Pressure Vessels & Piping Conf., July 27-31, 2008, Chicago, IL. Paper No. PVP2008-61552, http://www.asmeconferences.org/PVP08 (2008).

30. Fong, J. T., and Marcal, P. V., 2008a, "An Intelligent Flaw Monitoring System: From Flaw Size Uncertainty to Fatigue Life Prediction with Confidence Bounds in 24 Hours," Proc. 8th World Congress on Computational Mechanics, Venice, Italy, June 30-July 5, 2008, Ref. 1732, http://www.iacm-eccomascongress2008.org/ (2008a).

31. Fong, J. T., Hedden, O. F., and Lam, P. S., eds., 2008b, A Symposium Digest on Failure Prevention via Robust Design and Continuous NDE Monitoring, distributed free to July 31, 2008 symposium attendees and contributors at the ASME 2008 Pressure Vessels and Piping Division Conference, July 27-31, 2008, Chicago, IL. For further information, contact: fong@drexel.edu (2008b).

32. Fong, J. T., Hedden, O. F., Filliben, J. J., and Heckert, N. A., 2008c, "A Web-based Data Analysis Methodology for Estimating Reliability of Weld Flaw Detection, Location, and Sizing," Proc. ASME Pressure Vessels & Piping Conf., July 27-31, 2008, Chicago, IL. Paper No. PVP2008-61612, http://www.asmeconferences.org/PVP08 (2008c).

33. Fong, J. T., Ranson, W. F., III, Vachon, R. I., and Marcal, P. V., 2008d, "Structural Aging Monitoring via Web-based Nondestructive Evaluation Technology," Proc. ASME Pressure Vessels & Piping Conference, July 27-31, 2008, Chicago, IL. Paper No. PVP2008-61607,

http://www.asmeconferences.org/PVP08 (2008d).

34. Khaleel, M. A., and Simonen, F. A., 2008, Evaluations of Structural Failure Probabilities and Candidate Inservice Inspection Programs, a Pacific Northwest National Laboratory Report PNNL-13810 dated Nov. 2008 to appear as a NUREG document of U.S. Nuclear Regulatory Commission, Washington, DC 20555-0001 (2008).

35. Lydell, B.O.Y. and Olsson, A., 2008a, "Reliability Data for Piping Components in Nordic Nuclear Power Plants "R-Book" Project Phase I Rev 1", SKI Report 98:20, Swedish Nuclear Power Inspectorate, Stockholm, Sweden, (2008).

36. Lydell, B., Huerta, A., and Gott, K., 2008b, "Characteristics of Damage & Degradation Mechanisms in Nuclear Power Plant Piping Systems," Proc. ASME Pressure Vessels & Piping Conference, July 27-31, 2008, Chicago, IL. Paper No. PVP2008-61914,

http://www.asmeconferences.org/PVP08 (2008b).

37. Marcal, P. V., and Fong, J. T., 2008, "Continuous NDE Monitoring via Web Technology," Proc. ASME Pressure Vessels & Piping Conference, July 27-31, 2008, Chicago, IL. Paper No. PVP2008-61574,

http://www.asmeconferences.org/PVP08 (2008).

38. Pietrangelo, A. R., 2008a, Congressional testimony before the U.S. Senate Committee on Environment and Public Works, Subcommittee on Clear Air and Nuclear Safety, Washington, DC, July 16, 2008. Nuclear Energy Institute, Washington, DC 20006-3708,

http://www.nei.org/newsandevents/speechesandtestimony/2008_speeches_and_testimony/pietrangelo.html (2008a).

39. Pietrangelo, A. R., 2008b, Planning for Success: Reasoned Expectations for New Nuclear Plant Construction, a plenary lecture delivered at the ASME 2008 Pressure Vessels and Piping Conference, July 28, 2008, Chicago, IL. Nuclear Energy Institute, Washington, DC 20006-3708, http://www.nei.org (2008b).

40. Teather, D., 2004, "US nuclear industry powers back into life," The Guardian, Tuesday, 13 April 2004. http://www.guardian.co.uk (2004).

41. Cooper, M., 2009, "U.S. Infrastructure Is in Dire Straits, Report Says," New York Times, Jan. 28, 2009, page A16 (2009).

42. Allegheny County, 1999, "Jonathan Hulton Bridge," Bridges & Tunnels of Allegheny County & Pittsburgh, PA , http://pghbridges.com/newkenW/0597-4486/hulton.html (1999).

43. Box, G. E., Hunter, W. G., and Hunter, J. S., 1978, Statistics for Experimenters: An Introduction to Design, Data Analysis, and Model Building. Wiley (1978).

44. Croarkin, C., Guthrie, W., Heckert, N. A., Filliben, J. J., Tobias, P., Prins, J., Zey, C., Hembree, B., and Trutna, eds., 2006, NIST/SEMATECH e-Handbook of Statistical Methods, Chapter 5 on Process Improvement (pp. 1-480), http://www.itl.nist.gov/div898/handbook/, first issued, June 1, 2003, and last updated July 18, 2006. Produced jointly by the Statistical Engineering Division of the National Institute of Standards & Technology, Gaithersburg, MD, and the Statistical Methods Group of

SEMITECH, Austin, TX. Also available as a NIST Interagency Report in a CD-ROM upon request to alan.heckert@nist.gov (2006).

45. Filliben, J. J., and Heckert, N. A., 2002, DATAPLOT: A Statistical Data Analysis Software System, A Public Domain Software by NIST, Gaithersburg, MD 20899, http://www.itl.nist.gov/div898/software/dataplot.html (2002).

46. Fong, J. T., Filliben, J. J., deWit, R., Fields, R. J., Bernstein, B., and Marcal, P. V., 2006a, "Uncertainty in Finite Element Modeling and Failure Analysis: A Metrology-Based Approach," ASME Trans., J. Press. Vess. Tech., Vol. 128, pp. 140-147 (2006a).

47. Fong, J. T., Filliben, J. J., deWit, R., and Bernstein, B., 2006b, "Stochastic Finite Element Method (FEM) and Design of Experiments for Pressure Vessel and Piping (PVP) Decision Making," Proc. of 2006 ASME Pressure Vessels and Piping Division Conference, July 23-27, 2006, Vancouver, B. C., Canada, paper no. PVP2006-ICPVT11-93927. New York, NY: American Society of Mechanical Engineers (2006b)..

48. Fong, J. T., Filliben, J. J., Heckert, N. A., and deWit, R., 2008, "Design of Experiments Approach to Verification and Uncertainty Estimation of Simulations Based on Finite Element Method," Proc. Conf. Amer. Soc. for Engineering Education, June 22-25, Pittsburgh, PA, Paper AC 2008-2725 (2008).

49. Fong, J. T., deWit, R., Marcal, P. V., Filliben, J. J., and Heckert, N. A., 2009, "A Design-of-Experiments Plug-In for Estimating Uncertainties in Finite Element Simulations," to appear in Proceedings of 2009 International SIMULIA Conference, May 18-21, 2009, London, U.K., Paper ID 9098. Providence, RI: SIMULIA-Dassault Systemes Simulia Corp. (2009).

50. Marcal, P. V., Fong, J. T., and Yamagata, N., 2009, "Artificial Intelligence (AI) Tools for Data Acquisition and Probability Risk Analysis of Nuclear Piping Failure Databases," to appear in Proc. ASME Pressure Vessels & Piping Conference, July 26-30, 2009, Prague, The Czech Republic, Paper No. PVP2009-77871,

http://www.asmeconferences.org/PVP09 (2009a).

51. Fong, J. T., Marcal, P. V., Hedden, O. F., Chao, Y. J., and Lam, P. S., 2009a, "A Web-based Uncertainty Plug-In (WUPI) for Fatigue Life Prediction based on NDE Data and Fracture Mechanics Analysis," to appear in Proc. ASME Pressure Vessels & Piping Conference, July 26-30, 2009, Prague, The Czech Republic, Paper No. PVP2009-77827, http://www.asmeconferences.org/PVP09 (2009a).

52. Fong, J. T., and Marcal, P. V., 2009b, "A Dataplot-Python-Anlap (DPA) Plug-In for High Temperature Mechanical Property Databases to Facilitate Stochastic Modeling of Fire-Structure Interactions," to appear in Proc. ASME Pressure Vessels & Piping Conference, July 26-30, 2009, Prague, The Czech Republic, Paper No. PVP2009-77867, http://www.asmeconferences.org/PVP09 (2009b).

53. Marcal, P. V., 2009, ANLAP User's Manual. Published by MPACT Corp., Julian CA, marcalpv@cox.net (2009).

54. Schank, R., 1972, "Conceptual dependency: A theory of natural language understanding," Cognitive Psychology, Vol. 3 (4), pp. 552-631 (1972).

55. Schank, R. C., 1973, "Identification of Conceptualizations Underlying Natural Language," in Computer Models of Thought and Language, R. C. Schank and K. M. Colby, eds., Chapter 5. San Francisco, CA: W. H. Freeman and Company (1973).

56. Chamberlin, D. D., and Boyce, R. F., 1974, "SEQUEL: A Structural English Query Language," Proc. 1974 ACM SIGFIDET Workshop on Data Description, Access and Control, pp. 249-264. Association for Computing Machinery (1974).

57. ANSI/ISO/IEC 9075-2:1999, International Standard (IS), Information Systems -- Database Language -- SQL -- Part 2: Foundation (SQL/Foundation), 1147pp (1999).

58. ISO/IEC 9075-11: 2008, Information technology -- Database languages -- SQL -- Part 11: Information and Definition Schemas (SQL/Schemata), 278pp (2008)

59. Fong, J. T., 1983, "Access to Materials Data - The Future," in Computerized Materials Data Systems, Proc. 1982 NBS-CODATA Workshop, Fairfield Glade, Tennessee, pp. 111-114 (1983).

60. Fong, J. T., 1983, "Computer Software Needs of Material Property Databases for Selected Engineering Applications," in ASME Spec. Pub. MPC-20, pp. 75-105 (1983).

61. Fong, J. T., ed., 1984, Engineering Databases: Software for On-Line Applications, Spec. Pub. PVP-96. American Society of Mechanical Engineers, New York, NY (1984).

62. Fong, J. T., 1986, "Integration of Engineering Analysis and Databases for Critical Decision Making," Computers in Mechanical Engineering (CIME), Vol. 5, No. 1, pp. 42-55 (1986).

63. Bernstein, B., and Fong, J. T., 1991, "A PC-based Expert System Tool for Managing Materials Property Data," Proc. Post-Conf. Seminar on Expert Systems and AI Applications in the Power Generation Industry, 11th International Conf on Structural Mechanics in Reactor Technology (SmiRT-11), Tokyo, Aug. 26-27 (1991).

64. Ren, W., and Swindeman, R. W.l, 2005, Assessment of Existing Alloy 617 Data for Gen IV Materials Handbook, ORNL/TM-2005/510, U. S. Department of Energy Generation IV Nuclear Reactor Program, U. S. Department of Energy, (2005).

65. Ren, W., and Rittenhouse, P., 2005, “Construction of Web-Accessible Materials Handbook for Generation IV Nuclear Reactors”, Proc. of the 2005 ASME PVP Conference, PVP2005-71780, ASME, Denver, CO, USA, (2005).

66. Ren, W., 2008, "Development of Digital Materials Database for Design and Construction of New Power Plants," Proceedings of ICAPP '08, Anaheim, CA, June 8-12, 2008, Paper 8019 (2008).

67. Interrante, C. G., and Hicho, G. E., 1973, "Fracture Toughness Evaluation of Quenched-and-Tempered Bridge Steels," U. S. National Bureau of Standards Report NBSIR 73-293, Oct. 1973. National Technical Information Service, Springfield, VA 22161 (1973).

68. Interrante, C. G., Fong, J. T., Filliben, J. J., and Heckert, N. A., 2008, "Uncertainty Estimate of Charpy Data using a 5-factor 9-run Design of Experiments," Proc. ASME PVP Conference, July 27-31, 2008, Chicago, IL, Paper No. PVP2008-61565. New York, NY: ASME

http://www.asmeconferences.org/PVP08 (2008).

69. Chao, Y. J., Fong, J. T., and Lam, P. S., 2008, "A New Approach to Assessing the Reliability of Applying Laboratory Fracture Toughness Test Data to Full-Scale Structures," Proc. ASME Pressure Vessels & Piping Conference, July 27-31, 2008, Chicago, IL, Paper No. PVP2008-61584. New York, NY: ASME

http://www.asmeconferences.org/PVP08 (2008).

70. Gerberich, W. W., and Moody, N. R., 1979, "A Review of Fatigue Fracture Topology Effects on Threshold and Growth Mechanisms," in Fatigue Mechanisms, Proceedings of an ASTM-NBS-NSF symposium, Kansas City, MO, May 1978, J. T. Fong, Ed., ASTM STP 675, pp. 292-341. American Society for Testing and Materials, 100 Barr Harbor Dr., West Conshohocken, PA 19428-2959 (1979).

71. Cheverton, P. D., Canonico, D. A., Iskander, S. K., Bolt, S. E., Holtz, P. P., Nanstad, R. K., and Stelzman, W. J., 1983, "Fracture Mechanics Data Deduced from Thermal Shock and Related Experiments with LWR Pressure Vessel Material," Journal of Pressure Vessel Technology, Vol. 105, pp. 102-110 (1983).

72. Sherry, A. H., Lidbury, D. P. G., and Beardsmore, D.W., 2001, "Validation of Constraint-Based Structural Integrity Assessment Methods, Final Report," Report No. AEAT/RJCB/RD01329400/R003, AEA Technology, U.K. (2001).

73. NRIM, 1994, "Data Sheets on the Elevated Temperature Properties of High Strength Steel (Class 590 MPa) Plates for Pressure Vessels," NRIM Creep Data Sheet, Second Revised (No. 25B), 30 September 1994. Tokyo: National Research Institute for Metals (1994).

XIV. ACKNOWLEDGMENT

We wish to thank

Howard Baum, **Ron Boisvert, Robert Chapman, Robert Cook, Christopher Dabrowski, Nicholas Dagalakis, Alden Dima, Richard Fields, Elizabeth Fong**, **Edwin Fuller, John Gross, Raghu Kacker**, **Ma Li, Hung-Kung Liu**, **Bruce Miller, Anne Plant**, **Kuldeep Prasad, Ronald Rehm**, **Emil Simiu**, and **Sheldon Wierderhorn** of U. S. National Institute of Standards and Technology (NIST), Gaithersburg, MD, and **Andrew Dienstfrey** of NIST, Boulder, CO,

H. Norman Abramson (*retired*) of Southwest Research Institute, San Antonio, TX,

Barry Bernstein (*retired*) of Departments of Mathematics and Chemical and Environmental Engineering, Illinois Institute of Technology, Chicago, IL,

Hal Brinson (*retired*) of Department of Mechanical Engineering, University of Houston, Houston, TX,

Spencer Bush (*retired*), **Steven Doctor** and **Fredric Simonen** (*retired*) of Pacific Northwest National Laboratory, Richland, WA,

Borchin Chang, Bradley Layton, Alan Lau, and **Jack Zhou** of Department of Mechanical Engineering and Mechanics, Drexel University, Philadelphia, PA.

Y. J. (Bill) Chao and **William (Bill) Ranson** of Department of Mechanical Engineering, University of South Carolina, Columbia, SC,

Fu Liiong (Bill) Cho of Risk Solver Communications, Inc., Irvine, CA,

Alan Chockie of Chockie Group International, Seattle, WA,

I-Ling Chow (*retired*) of U.S. Department of Energy, Germantown, MD,

Marvin Cohn and **Geoffrey Egan** of Aptech Engineering Services, Sunnyvale, CA,

Owen Hedden of Codes & Standards Consulting, Fort Worth, TX,

Jon Helton and **Willliam Oberkampf** of Sandia National Laboratory, Albuquerque, NM,

Charles Interrante *(retired)* of U.S. Nuclear Regulatory Commission, Washington, DC,

Mel Kanninen of San Antonio, TX,

Poh-Sang Lam of Savannah River National Laboratory, Aiken, SC,

Bengt Lydell of Scandpower Risk Management, Inc., Houston, TX,

Andrew MacKeith and **David Winkler** of Dassault Systemes Simulia Corp., Providence, RI,

Paul Mitiguy and **Charles Steele** (*retired*) of Department of Mechanical Engineering, Stanford University, Stanford, CA,

Anthony Pietrangelo of Nuclear Energy Institute, Washington, DC,

Robert Rainsberger of XYZ Scientific Applications, Inc., Livermore, CA,

Robert Reid of RHR Consulting Engineers, Oakmont, PA,

Weiju Ren and **Robert Swindeman** (*retired*) of Oak Ridge National Laboratory, Oak Ridge, TN,

T. Richard (Dick) Robe (*retired*) of College of Engineering, Ohio University, Athens, OH,

Glenn Sinclair of Department of Mechanical Engineering, Louisiana State University, Baton Rouge, LA,

Reginald Vachon of Direct Measurement, Inc., Atlanta, GA, and

Tomasz Wierzbicki of Department of Mechanical Engineering, Massachusetts Institute of Technology, Cambridge, MA,

for their valuable discussions, comments, and/or technical assistance during the course of our investigation that began by one of our co-authors (**Fong**) thirty years ago shortly after the Three Mile Island accident.

APPENDIX A

The following is an abbreviated version of the output file created by the PC-PRAISE code after we submit a typical input data sheet named X230.DAT:

```
               P      R           A        I         S       E

             PIPING RELIABILITY ANALYSIS INCLUDING SEISMIC EVENTS
                          PC-PRAISE VERSION 4.42
                       EXECUTED ON  03/17/2009 AT    8:53p
                    ECHO-PRINT OF INPUT DATA IN FILE  X230.DAT
================================================================================================
    1>HOT-LEG FILE=HL0X23  PROB-CALC  SIM=10^4   90 CRKS
    2>    3    0   90   -4         0     1.100         0   14    688    7225    0    0
    3> -100    1    2    0 -0.2    0    0    0    0    0    0    0    0    0    0    0
    4>         0      .015      0.01     0.118    0.0789    0.0001    0    0       1.0
    5>      60.0  .200E+00    0    0
    6>     2.500     14.50      10.0
    7>      8.19      1.16 6.327E-07 1.141E-06       1.0
    8> .3970E+02 .3970E+01      10.0      25.0      19.4     106.0   25800.0      5.00
    9>      60.0       6.0    0
   10>  .100E+01  .500E+02                         -3.50     -1.20
   11>      2.08      8.58     2.250     -3.00  .100E+01  .000E+00
   12>    6    9  100  100
   13>      .010      .100      .200      .300      .400      .500      .600      .700
   14>      .800
   15>     1.000     2.000     3.000     4.000     5.000     6.000
   16>    1      20.0 600. HEAT-UP AND COOL-DOWN
   17>   .001000         1
   18> 1000    .00008 590. # 1  HIGH-STR/LOW-CYCLE  SEE NOTES BELOW 500000 CYCLES/40 Y
   19>   .001000         2    37.790
   20>     0.0     0.0     0.0     0.0     0.0     0.0     0.0     0.0     0.0
   21>     0.0     0.0     0.0     0.0     0.0     0.0     0.0     0.0     0.0
   22>     0.0     0.0     0.0     0.0     0.0     0.0     0.0     0.0     0.0
   23>     0.0     0.0     0.0     0.0     0.0     0.0     0.0     0.0     0.0
   24>     0.0     0.0     0.0     0.0     0.0     0.0     0.0     0.0     0.0
   25>     0.0     0.0     0.0     0.0     0.0     0.0     0.0     0.0     0.0
   26>  42.899  28.242  18.601  13.832  12.454  13.194  15.142  17.920  21.512
   27>  54.252  37.518  26.443  20.744  18.732  19.117  21.048  24.061  28.171
   28>  58.761  40.702  28.939  23.263  21.571  22.498  25.262  29.486  35.263
   29>  60.842  41.666  29.837  24.392  23.022  24.444  27.898  33.082  40.182
   30>  62.461  42.846  30.855  25.402  24.141  25.728  29.416  34.878  42.342
   31>  63.366  43.470  31.446  26.097  25.014  26.834  30.825  36.755  44.843
   32>     0.0     0.0     0.0     0.0     0.0     0.0     0.0     0.0     0.0
   33>     0.0     0.0     0.0     0.0     0.0     0.0     0.0     0.0     0.0
   34>     0.0     0.0     0.0     0.0     0.0     0.0     0.0     0.0     0.0
   35>     0.0     0.0     0.0     0.0     0.0     0.0     0.0     0.0     0.0
   36>     0.0     0.0     0.0     0.0     0.0     0.0     0.0     0.0     0.0
   37>     0.0     0.0     0.0     0.0     0.0     0.0     0.0     0.0     0.0
   38>  46.068  36.848  29.280  24.065  20.688  18.677  17.622  17.242  17.351
   39>  48.029  37.276  29.397  24.577  21.913  20.808  20.918  21.973  23.924
   40>  48.060  37.052  29.264  24.633  22.227  21.416  21.880  23.381  25.916
   41>  48.478  37.520  29.799  25.192  22.647  21.753  22.086  23.436  25.716
   42>  48.351  37.416  29.715  25.213  22.960  22.357  23.076  24.865  27.760
   43>  48.250  37.302  29.615  25.139  22.953  22.377  23.108  24.969  28.021
   44>
   45>
   46>STRESS - RESIDUAL STRESS IS MAXIMUM RESIDUAL STRESS IN WELD/BUTTER
   47>
   48>DA/DN CONSTANT C PER PROLOCA VALUE FOR A182. The final paragraph of Section 2.8.
   49>talks about Alloy 182 at 325C (617F).  The log-mean of C is given as -25.47
   50>the log-standard deviation of C is stated as 0.46. The mean crack growth rate at
   51>da/dt=8.6800x10-12(K-9.0)^1.16 where da/dt in meter/sec and K in MPaSqrt(meter)

================================================================================================
```

APPENDIX A (CONT'D)

```
      --- HOT-LEG FILE=HL0X23  PROB-CALC  SIM=10^4   90 CRKS                          ---

      CIRCUMFERENTIAL CRACK ANALYSIS

      PARAMETERS FOR PSI NON-DETECTION PROBABILITY
          EPST  =     .000E+00
          ASTAR =    1.250
          TRANSDUCER DIAMETER =  1.00000 INCHES
          ANUU  =    1.600
     ISI NON-DETECTION PARAMETERS SAME AS FOR PSI
      FATIGUE-INITIATED CRACKS ONLY
      MAXIMUM NO. OF CRACKS =   90
      NO. OF REPLICATIONS   =     10000
      A/H BOUNDARY          =    1.1000
          Sampling around the circumference - independent
          sampling around circumference based zero correlation
          Crack growth independent of initiation

      FATIGUE CRACK GROWTH ONLY
                        MATERIAL SELECTED - S316NG
                        WATER ENVIRONMENT
      LEAKERS WILL NOT BE REPAIRED

      FAILURE CRITERIA = APPLIED STRESS>FLOW STRESS

      PIPE DIMENSIONS
          WALL THICKNESS =   2.50 INCHES
          INSIDE RADIUS  =  14.50 INCHES
            L/H RATIO    =    58.00
            L/R RATIO    =    10.00
          AREA OF PIPE         =   247.40 SQ. INCHES
          FLOW AREA OF PIPE    =   660.52 SQ. INCHES

      CRACK GROWTH LAW PARAMETERS
          EXPONENT  =   1.160
          GROWTH LAW CONSTANT LOG-NORMALLY DISTRIBUTED
               MEDIAN        =   .6327E-06
               90-TH PERCENT =   .1141E-05
          THRESHOLD =   8.190

      FATIGUE-INITIATION PARAMETERS
                      SULFUR (WEIGHT %) =  .01500
                  DISSOLVED OXYGEN(PPM) =  .01000
              Initiated Crack Depth(in) =    .118

                  Median (b-a),(in) = .078900
                      SD of ln(b-a) = .000100
          Initiation time multiplier    =   1.000

 SNFACTOR =        1.000000

      FLOW STRESS NORMALLY DISTRIBUTED
          MEAN                =   .3970E+02
          STANDARD DEVIATION =   .3970E+01

      DISTRIBUTION PARAMETERS FOR ULTIMATE STRESS IN PIPE
          MEAN                =   .6000E+02
          STANDARD DEVIATION =   .6000E+01
          STANDARD DEVIATION =  0.0 MEANS THE ULTIMATE STRESS IS CONSTANT
          INTERPOLATION FLAG =   0  ( IULT ) FOR WHOLE PIPE BREAK PROBABILITY
          ABS ( IULT ) IS THE NUMBER OF INTERPOLATION POINTS
          IF  IULT .GT. 0  LINEAR INTERPOLATION
          IF  IULT .EQ. 0  NO INTERPOLATION
          IF  IULT .LT. 0  LOGARITHMIC INTERPOLATION
```

M2: crack growth law exponent (m)

N2: crack shape ellipticity (b-a)

M5: mean flow stress

M6: Ultimate tensile

```
        JIC (IN-KIPS/IN.IN) =     10.0000
            DJDA      (KSI) =     25.0000
        YIELD STRESS  (KSI) =     19.4000
               D      (KSI) =    106.0000
        YOUNGS MODULUS(KSI) =  25800.0000
        EXPONENT, N         =      5.0000

    PIPE LOADING VALUES
        STRESS (KSI) DUE TO COLD DEADWEIGHT  =     2.08
        STRESS (KSI)  DUE TO DWGHT + THERMAL =     8.58
        STRESS (KSI)  DUE TO         THERMAL =     6.50
        OPERATING PRESSURE (KSI)             =     2.25
        STRESS (KSI) DUE TO OPER. PRESSURE   =     6.01
        STRESS (KSI) DUE TO DWGHT + OP PRESR =     8.09
        STRESS (KSI) DUE TO DWT+THML+OP PRES =    14.59

        NO HYDROSTATIC PROOF TEST IS MODELLED
        VIBRATORY STRESSES (KSI)             =     1.00
        VIBRATIONAL THRESHOLD (R-STAR)       =      .00

    LEAK DETECTION AND DEFINITION PARAMETERS
        DETECTABLE LEAK (GPM) =    1.00
        BIG LEAK        (GPM) =   50.00
        Pathway Loss Coeff.   =    3.00
        Crack Roughness (in)  =.0002441

    NO RESIDUAL STRESSES ARE MODELLED
    VIBRATORY STRESSES ARE MODELLED
    NO PRE-SERVICE ULTRASONIC INSPECTION
================================================================
    NO IN-SERVICE INSPECTIONS ARE MODELLED
    NO SEISMIC EVENTS EVALUATED
   SKIP PARAMETER FOR INDICATOR FUNCTION PRINTOUT IS   0
    NORMAL OUTPUT REQUESTED

    NUMBER OF TRANSIENT TYPES =  2
    TYPE  1     HEAT-UP AND COOL-DOWN
        REGULAR AT        20.0000000000 YEARS/EVENT
        MAX DELTA TEMP = 600.0
        BLOCKING FACTOR =     1.00000000
        Transient Type 1: Uniform stress
        Strain Rate 1.0000E-03
        Uniform Stress range at ID (ksi) =      12.51
        Bending Stress range at ID (ksi) =        .00
        Gradient Stress range at ID (ksi) =        .00
        Total surface stress (ksi)        =      12.51
    TYPE  2     # 1  HIGH-STR/LOW-CYCLE  SEE NOTES BELOW 500000
        REGULAR AT          .0000800000 YEARS/EVENT
        MAX DELTA TEMP = 590.0
        BLOCKING FACTOR =  1000.00000000
        Transient Type 4: tiffany Table
        Strain Rate 1.0000E-03
        Uniform Stress range at ID (ksi) =      37.79
        Bending Stress range at ID (ksi) =        .00
        Gradient Stress range at ID (ksi) =        .00
        Total surface stress (ksi)        =      37.79

        ** Critical crack sizes input by the user **
         Critical crack size for leaks:
         INTIME    Big Leak     Detectable Leak
            1       3.5000 in       1.2000 in

                          - - - UNIFORM MESH - - -
```